

Research Paper

A Novel MPEG-PDLLA-PLL Copolymer for Docetaxel Delivery in Breast Cancer Therapy

Liwei Tan, Jinrong Peng, Qian Zhao, Lan Zhang, Xichuan Tang, Lijuan Chen, Minyi Lei, Zhiyong Qian 

State Key Laboratory of Biotherapy and Cancer Center, Collaborative Innovation Center of Biotherapy, West China Hospital, Sichuan University, Sichuan, China

 Corresponding author: Tel/Fax: +86-28-85501986, E-mail: anderson-qian@163.com© Ivyspring International Publisher. This is an open access article distributed under the terms of the Creative Commons Attribution (CC BY-NC) license (<https://creativecommons.org/licenses/by-nc/4.0/>). See <http://ivyspring.com/terms> for full terms and conditions.

Received: 2017.02.15; Accepted: 2017.04.27; Published: 2017.07.06

Abstract

Satisfactory drug loading capacity and stability are the two main factors that determine the anti-cancer performance. In general, the stability of the micelles is reduced when the drug loading (DL) is increased. Therefore, it was a challenge to have high drug loading capacity and good stability. In this study, we introduced a hydrophilic poly (L-Lysine) (PLL) segment with different molecular-weights into the monomethoxy poly (ethylene glycol)-poly (D, L-lactide) (MPEG-PDLLA) block copolymer to obtain a series of novel triblock MPEG-PDLLA-PLL copolymers. We found that the micelles formed by a specific MPEG_{2k}-PDLLA_{4k}-PLL_{1k} copolymer could encapsulate docetaxel (DTX) with a satisfactory loading capacity of up to 20% (w/w) via the thin film hydration method, while the stability of drug loaded micellar formulation was still as good as that of micelles formed by MPEG_{2k}-PDLLA_{1.7k} with drug loading of 5% (w/w). The results from computer simulation study showed that compared with MPEG_{2k}-PDLLA_{1.7k}, the molecular chain of MPEG_{2k}-PDLLA_{4k}-PLL_{1k} could form a more compact funnel-shaped structure when interacted with DTX. This structure favored keeping DTX encapsulated in the copolymer molecules, which improved the DL and stability of the nano-formulations. The *in vitro* and *in vivo* evaluation showed that the DTX loaded MPEG_{2k}-PDLLA_{4k}-PLL_{1k} (DTX/MPEG_{2k}-PDLLA_{4k}-PLL_{1k}) micelles exhibited more efficiency in tumor cell growth inhibition. In conclusion, the MPEG_{2k}-PDLLA_{4k}-PLL_{1k} micelles were much more suitable than MPEG_{2k}-PDLLA_{1.7k} for DTX delivery, and then the novel nano-formulations showed better anti-tumor efficacy in breast cancer therapy.

Key words: Docetaxel micelles; polymeric micelles; interaction; anti-tumor; drug loading capacity.

Introduction

Nano-formulations have become a new kind of drug formulations which has overcome some of the critical problems of traditional drug forms, including drug hydrophobicity (which reduces the bioavailability), the auxiliary toxicity, etc [1-3]. Combining with enhanced permeability and retention (EPR) effect, passive targeting can be achieved in solid tumor therapy, which also enhances the bioavailability of the drugs [4, 5]. Up to date, more than 40 kinds of nano-formulations, which have been studied in clinical trial, and several of them have been launched into the market [6-8].

As the prototype microtubule stabilizers, taxanes has been widely applied in the treatment of patients

with breast, lung and gynecologic cancers [9]. As one kind of taxanes, DTX is a semi-synthetic analog of paclitaxel. Due to its poor solubility, low selective distribution and fast elimination, the use of DTX has been restricted [10]. Currently, the commercial formulations of DTX (Taxotere®) have been reported to cause serious side-effects due to DTX itself or polysorbate 80 [11]. Therefore, the studies of nano-formulations are used to overcome these disadvantages [12-14]. Passive targeting and active targeting that are the two main ways that accumulated drugs into tumor sites. To improve the biocompatibility of nano-formulations, PEG [15, 16] and D- α -tocopheryl polyethylene glycol 1000

succinate (TPGS) [17, 18] are often used as the surface of which. The DTX formulation based on MPEG-PDLLA copolymers micelles (Nanoxel-PM™) have been list in South Korea [19, 20]. TPGS, a water-soluble derivative of natural vitamin E, was used for drug delivery as a multirole excipient. Mei *et al.* modified PLGA or PLA with TPGS to enhance the biocompatibility of the DTX nanoparticles for cancer therapy [21-26]. As more and more nano-formulations have been developed and evaluated in pre-clinical trials, however, the results reveal that tumor targeting of the nano-formulations still need to be improved [27]. Although numerous tumor-targeting ligands, including antibodies, proteins ligands [28, 29], have been introduced to the nano-systems to achieve active targeting through receptor-mediated endocytosis (RME) [30], the protein corona and ligand dissociation still impede the targeting efficacy [31, 32]. Moreover, the stimuli-intelligent polymeric micelles, which are response to endogenous stimulations (pH, enzyme, reduction and oxidation) and exogenous stimulations (heat, light, ultrasound and magnetic field), have been regarded as candidate vehicles for DTX [33]. However, in the case of solid tumor, passive targeting is still determining the targeting efficacy of nano-formulations [34, 35]. Some previous researches have revealed that the passive targeting efficacy is affected by particle size, surface charge, the ratio of hydrophobic segment/hydrophilic segment, the stealth coating, etc [36-38]. All of these factors are connecting with the stability of the nano-formulations. Therefore, the stability of the nano-formulations has critical importance to the passive targeting, which is directly connected with the anti-cancer properties of the nano-formulations. Moreover, similar to drugs, many imaging substance are loaded into micelles as probes for biological imaging [39, 40]. Therefore, improving the stability of drug loaded micelles can also improve the construction of stable imaging agents.

On the other hand, achieving high drug loading capacity is also a challenge for the designs of efficient drug carriers. In generally, the DL of nano-formulations is not exceeded 10%, which may lead the patients to absorb abundant carrier materials [41]. So, satisfactory drug loading capacity and stability were the two main factors for an ideal nano-formulation. In our previous study, we have constructed a DTX loaded MPEG_{2k}-PDLLA_{1.7k} (DTX/MPEG-PDLLA) micellar nano-formulation which was used to inhibit the tumor growth [42, 43]. The DTX nano-formulation based on MPEG_{2k}-PDLLA_{1.7k} block polymer micelles, Nanoxel-PM™, (which is launched into the South Korea market) has solved its hydrophobicity and

reduced some undesired side-effects. However, its DL is only 5% [19, 20, 44]. And what's more, from its operating instruction manual, it must be used within 4 hrs after re-dissolved, which indicate this formulation will become instable after 4 hrs. And we also proved this assumption in our previous research [43]. In order to further enhance the stability of the DTX micellar nano-formulations, more suitable nano-carriers which not only can enhance the DL but also can enhance the stability of the DTX loaded nano-formulation are needed to be developed.

According to some reports, the introduction of charge segment to the polymer chain may help to enhance the stability of the nanoparticles [45, 46]. Lysine as a natural amino acid has good biocompatibility [47]. Some early reports indicated that PLL have some activity against murine tumors [48]. PLL also exhibits amount of unique membrane properties, which include the ability to enhance the cellular uptake of macromolecule. It is beneficial to the uptake of nano-formulations by tumor cells [49]. These effects might be related to the cationic property of PLL and specific interactions on cell membrane [50]. Nowadays, PLL has been exhibited the ability as an efficient drug and gene carrier for tumor therapy [51, 52]. Therefore, in this study, we intend to introduce the biodegradable and biocompatible PLL to the polymer chain of MPEG-PDLLA. After the introduction of PLL, a triblock polymer which was named as MPEG-PDLLA-PLL was achieved. However, the introduction of PLL might change the hydrophilic-hydrophobic property of MPEG-PDLLA. Thus, the effect of the molecular weight of the MPEG, PDLLA and PLL in MPEG-PDLLA-PLL molecular weight on the DL and stability needed to be optimized in detail.

So, in this study, we first synthesized a series of MPEG-PDLLA-PLL triblock polymers with different molecular weight and composition. Then, we further evaluated the DL and stability of DTX micelles formed by this series polymer. After optimization, a special DTX/MPEG_{2k}-PDLLA_{4k}-PLL_{1k} micellar nano-formulation was chosen and be further evaluated the association of DL or micellar stability and anticancer performance, shown in figure 1. Drug loading capacity of the DTX/MPEG_{2k}-PDLLA_{4k}-PLL_{1k} was evaluated by the determination of DL and drug release behavior in different environments. And in order to theoretical reveal the connection between polymer chemical composition-drug interaction and the stability of the drug loaded micelles; three dimensional (3D) model simulation was also introduced to simulative reproduce the formation process of the DTX/MPEG_{2k}-PDLLA_{4k}-PLL_{1k} micelles. The interaction energy between DTX and

MPEG_{2k}-PDLLA_{4k}-PLL_{1k} molecules could be obtained. Finally, we further evaluated the therapeutic effect of the DTX/MPEG_{2k}-PDLLA_{4k}-PLL_{1k} on breast cancer *in vitro* and *in vivo* in detail. All the results demonstrated that introduction of PLL could regulate the stability of DTX micellar nano-formulations, and MPEG_{2k}-PDLLA_{4k}-PLL_{1k} was also a promising candidate for DTX delivery.

Materials and Methods

Materials

MPEG-PDLLA copolymers were synthesized following the previous work of our group [42, 53]. N^ε-carboxybenzoxy-L-lysine (H-Lys (Z)-OH) and N-t-butoxycarbonyl-L-phenylalanine (Boc-L-Phe) and triphosgene were purchased from GL Biochem Co., Ltd (Shanghai, China). DTX was purchased from Sichuan Xieli Pharmaceutical Co., Ltd (Chengdu, China). DTX injection, as the free DTX group in this study, was supplied by Hengrui Medicine Co, Ltd (Jiangsu, China). Dehydrated alcohol (Aladdin, Shanghai, China), triphosgene (Sigma, USA)

acetonitrile (Sigma, USA), Roswell Park Memorial Institute 1640 medium (RPMI 1640, Gibco, USA) (1640), Dulbecco's modified Eagle's medium (DMEM, Sigma, USA) (DMEM) and 3-(4, 5-dimethylthiazol-2-yl)-2, 5-diphenyltetrazolium bromide (MTT, Sigma, USA) (MTT) were used without any further purification. Annexin V-FITC Apoptosis Detection Kit was obtained from Key Gen Biotech (Nanjing, China). 1, 1'-dioctadecyl-3, 3', 3'-tetramethylindotricarbocyanine (DiD) was purchased from Biotium (Hayward, CA). Ki-67 Rabbit Monoclonal Antibody was obtained from Labvision (Minneapolis, USA). DAPI and Coumarin-6 (C6) were obtained from Sigma-Aldrich (Saint Louis, USA). All the materials used in this article were analytical grade and used as received.

MCF-7 cell line, 4T1 cell line, HEK293 cells and HUVEC cells were obtained from the American Type Culture Collection (ATCC; Rockville, MD), and grown in DMEM media and 1640 media, respectively. The cell culture was maintained in a 37 °C incubator with a humidified 5% CO₂ atmosphere.

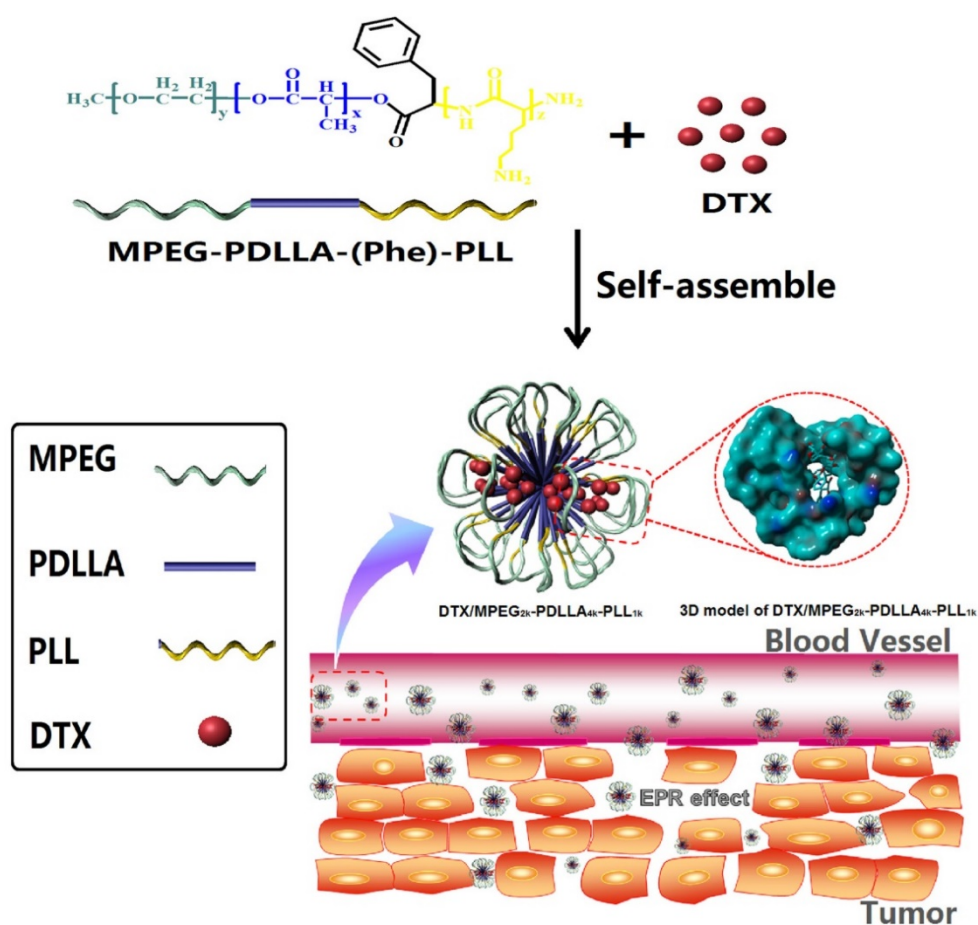


Figure 1. Structure and passive targeting mechanism of the DTX/MPEG_{2k}-PDLLA_{4k}-PLL_{1k}. The micelle was consisted of MPEG_{2k}-PDLLA_{4k}-PLL_{1k} and DTX. DTX and PDLLA as the hydrophobic part formed the core of micelles, and the shell of micelle was formed by hydrophilic segments MPEG and PLL. From the 3D model of DTX/MPEG_{2k}-PDLLA_{4k}-PLL_{1k}, DTX was completely wrapped in core of the copolymer. The accumulation of DTX/MPEG_{2k}-PDLLA_{4k}-PLL_{1k} in tumor tissue was through EPR effect.

Fifty-two Balb/c-nu mice and fifty Balb/c mice were used for antitumor tests, purchased from the HFk Bio-Technology Co., LTD (Beijing, China). All animal care and experimental procedures were conducted following the guidelines (IACUC-S200904-P001) approved by the Institutional Animal Care and Treatment Committee of Sichuan University (Chengdu, P.R. China). All the mice were treated humanely throughout the experimental period.

Synthesis of Lys (Z)-NCA

Synthesis of N-carboxyanhydride of 6-(benzyloxycarbonyl)-L-lysine (Lys (Z)-NCA) was carried out by the Fuchs-Farthing method using triphosgene as in the previous description [54]. Firstly, one dose of H-Lys (Z)-OH and half one dose of triphosgene were added to tetrahydrofuran (THF), and then the reaction mixture was heated to 50 °C while being stirred. The solvent was evaporated to terminate the reaction when the mixture became transparent. The product was purified in cold n-hexane three times. The structure of the Lys (Z)-NCA was characterized by Fourier Transform Infrared (FTIR) recorded on Nicolet 200SXV meter (Nicolet, USA).

Synthesis of MPEG-PDLLA-PLL

Firstly, MPEG-PDLLA was synthesized from the D, L-lactide, and MPEG by ring opening polymerization (ROP) in an environment of nitrogen with 130 °C oil bath for 8 hrs, and purified by precipitation in petroleum ether [53]. By connecting MPEG-PDLLA and Boc-Phe-OH, the amino end-group of MPEG-PDLLA was obtained after removing the t-butoxycarbonyl end group from Boc-L-Phe end-capped MPEG-PDLLA. And then, the MPEG-PDLLA-PLL was synthesized by the ROP with Lys (Z)-NCA through amino terminated MPEG-PDLLA, which was stirred in chloroform for 72 hrs. Finally, to get the MPEG-PDLLA-PLL triblock copolymer, the deprotection reaction of the copolymer MPEG-PDLLA-PLL was carried out in HBr/HAc solution. Purified MPEG-PDLLA-PLL was obtained by dialysis and freeze drying [55]. The structure of the polymer was characterized by nuclear magnetic resonance spectroscopy (¹H-NMR) (Varian 400 spectrometer, Varian, USA) and FTIR, the molecular weight was characterized by Gel Permeation Chromatography (GPC) (THF, 0.6 ml/min, Agilent 110 HPLC, America).

Preparation and characterization of the DTX micelles

The micelles were prepared by a thin film hydration method. Primarily, DTX and copolymers were co-dissolved in dichloromethane. Then the

solution was evaporated in a rotary evaporator at 60 °C, and the homogenous co-evaporation was obtained. Subsequently, the mixture was dissolved in double distilled water at 60 °C to self-assemble into micelles. Next the micelles were filtered through a 0.22 μm syringe filter (Millex-LG, Millipore Co., USA). Finally the micellar solution was freeze-dried to receive DTX micelle powder [56].

The particle size distribution and the zeta potential of the DTX micelles were determined by dynamic light scattering (DLS) (Malvern Nano-ZS 90, Malvern, UK). The morphology of the micelles could be detected by transmission electron microscopy (TEM). Crystallographic assay was performed on free DTX powder, blank MPEG_{2k}-PDLLA_{4k}-PLL_{1k} copolymer and DTX/MPEG_{2k}-PDLLA_{4k}-PLL_{1k} micelles though an X-ray diffractometer (XRD) (X'Pert Pro, Philips, Netherlands) using CuKα radiation. The data was assembled from step-scan mode from 5 ° to 50 ° with a step size of 0.03.

Drug loading capability of MPEG-PDLLA-PLL

The DL and entrapment efficiency (EE) of the micelles were determined by High Performance Liquid Chromatography (HPLC) (HPLC 1260, Agilent, US) with a C₁₈ column (4.6 mm × 150 mm × 5 μm, Grace Analysis column). The compositions of the mobile phase were Acetonitrile/ammonium acetate solution (45/55, v/v) at a flow rate of 1 ml/min. Detection was taken on a diode array detector (1260 DAD VL) at a wavelength of 232 nm. Before the measurement, the samples were diluted with acetonitrile [57]. The results were calculated using the following equations:

$$DL\% = \frac{\text{Amount of DTX determined in micelle}}{\text{Amount of DTX determined} + \text{copolymer}} \times 100\%$$

$$EE\% = \frac{\text{Amount of DTX determined in micelle}}{\text{Amount of DTX in feed}} \times 100\%$$

Evaluation of stability

To investigate the stability of the DTX micelles solution, the solution was stored at room temperature without lyophilization. The stability status was evaluated by macroscopic observation [58]. The DTX micelles solution was unstable while a precipitate could be seen clearly. This method was according to Chinese Pharmacopoeia 2010 (ChP 2010).

Molecular modeling study

The initial structures of MPEG_{2k}-PDLLA_{1.7k} and MPEG_{2k}-PDLLA_{4k}-PLL_{1k} were constructed using Moltemplate, which was a general cross-platform text-based molecule builder for LAMMPS (Large-scale Atomic/Molecular Massively Parallel Simulator) [59], and optimized by the force field

method. Then the DTX molecule was docked to the simulated copolymers to construct the micelle, randomly. The molecular dynamic (MD) simulation was calculated in a Compass force field [60]. The temperature coupling and pressure coupling of the MD simulation were determined by Nose-Hoover and Berendsen, respectively. The MD simulation process was as follows: The initial temperature of the system was set from 0 K to 600 K, the step size was 0.5 fs and the step number was 200000. The simulated annealing was performed while the system temperature reached the set value, and then the system temperature was cooled to 300 K within 100 ps. The equilibrium molecular dynamics simulation of isothermal-isobaric ensemble (NPT) was performed after the annealing treatment [61]. The PyMol was used for visual analysis [62].

In order to explore the mechanism of the copolymers entrapping DTX, the interaction between DTX and the copolymers was investigated. The interaction energy was calculated according to the following equation. The results were listed in Table 2 [63, 64].

$$\Delta E_{\text{interaction}} = E_{\text{complex}} - E_{\text{copolymer}} - E_{\text{docetaxel}}$$

Drug release behavior of the micelles *in vitro*

The drug release behaviors of the DTX micelles in different pH environments were evaluated by using the dialysis method. Briefly, free DTX, DTX/MPEG_{2k}-PDLLA_{1.7k} micelles and DTX/MPEG_{2k}-PDLLA_{4k}-PLL_{1k} micelles were separately suspended in a dialysis bag (molecular weight cutoff: 14k Da) and were then immersed into different pH PBS solution at 37 °C under horizontal shaking (100 rpm/min). At predetermined intervals, the aliquots (2 ml) were withdrawn and replaced by the same amount of PBS. The amount of DTX released at designated time points were measured by HPLC. The chromatographic conditions and the methods followed determination of DL.

To investigate the stability of the DTX/MPEG_{2k}-PDLLA_{4k}-PLL_{1k} micelles, the DTX/MPEG_{2k}-PDLLA_{4k}-PLL_{1k} micelles were stored at room temperature. The sample was filtered to remove the leaked DTX at predetermined time points, and the content of DTX remaining in the micelles solution was measured by HPLC according to United States Pharmacopeia (USP).

Hemolysis test

The hemolytic potential of the MPEG_{2k}-PDLLA_{4k}-PLL_{1k} micelles *in vitro* was tested as follows: Rabbit blood without fibrinogen was washed and diluted with normal saline to get a suspension of 2% red blood cells (RBCs). 2.5 ml of micelles with

different concentrations were added to 2.5 ml of the RBCs suspension. Distilled water and normal saline were added to the RBC suspension as positive and negative controls, respectively. All samples were incubated at 37 °C for 3 hrs and then centrifuged. The absorbance of supernatant was determined at 545 nm by UV/VIS Spectrometer (Lambda 35, Perkin Elmer). When this value was greater than 5%, the sample possessed hemolytic potential. The hemolytic rate was calculated according to the following equations:

$$\text{Hemolytic Rate} = (\text{OD}_{\text{sample}} - \text{OD}_{\text{negative}}) / (\text{OD}_{\text{positive}} - \text{OD}_{\text{negative}}) \times 100\%$$

Delivery of the micelles *in vitro*

DTX was replaced by a hydrophobic fluorescent probe C6 to investigate the cellular uptake of micelles. For fluorescence microscopy observation, MCF-7 cells and 4T1 cells were incubated for 24 hrs in 6-well plates (2×10⁴ cells per well) at 37 °C. The C6/MPEG_{2k}-PDLLA_{4k}-PLL_{1k} micelles, C6/MPEG_{2k}-PDLLA_{1.7k} micelles and free C6 were added to the plates at the final concentration of C6 was 100 ng/ml, respectively. And then the cells were washed with PBS after fixing with 4% paraformaldehyde in PBS. Subsequently, the fixed cells were treated with DAPI for 5 min, and then the fluorescence images of the micelles cellular uptake was observed under a fluorescence microscope; (Olympus, China) with excitation at 488 nm. For flow cytometry analysis, the cells (3×10⁵ cells per well) incubated for 24 hrs in 6-well plates at 37 °C, and then were treated with the normal saline (NS) as control, C6/MPEG_{2k}-PDLLA_{4k}-PLL_{1k} micelles, C6/MPEG_{2k}-PDLLA_{1.7k} micelles and free C6 in 6-well plates as described above. The cells were harvested in PBS after treated with Trypsin-EDTA, and the fluorescence intensity of the cells was determined by an ACEA NovoCyte™ Flow Cytometer (NovoExpress™, ACEA Bioscience, Inc., USA)

Evaluation of cytotoxicity *in vitro*

MTT assay

Firstly, the cells (3×10³ cells/well) were cultured in 96-well plates and incubated for 24 hrs at 37 °C. Micelles of different concentrations were added and cultivation continued for 24 hrs. 20 μl MTT solution (5 mg/ml) was added into each well, and the MTT solution was removed and replaced with DMSO (160 μl/well) after 3 hrs. The absorbance was measured at a wavelength of 490 nm using a 680 model microplate reader from an infinite M200 microplate reader (Tecan, Durham, USA).

Cell apoptosis analysis

Cells were seeded into 6-well plates at 2×10⁵

cells/well. The different DTX formulations were added at the dosage of 10 µg DTX per ml and incubated for 24 hrs. The cells were collected and washed three times in normal saline. The cells were resuspended in a binding buffer, and Annexin V-FITC and PI were added in sequence. The cells were analyzed by the flow cytometry

Delivery of the micelles *in vivo*

In order to eliminate the artifact signal caused by the fur of the Balb/c-nu mice during bioluminescence imaging, the Balb/c-nu mice were chosen as the experimental subject. MCF-7 cells ($2 \times 10^6/0.1$ ml) were incubated in the right flank of the athymic female BALB/c-nu mice by a subcutaneous injection. The near-infrared fluorescence dye DID was used to replace DTX as the fluorescence probe to be encapsulated in the micelles to evaluate the bio-distribution *in vivo*. The mice were divided into control group, free DID group, DID/MPEG_{2k}-PDLLA_{1.7k} group and DID/MPEG_{2k}-PDLLA_{4k}-PLL_{1k} group, which was treated with NS as control, free DID, DID/MPEG_{2k}-PDLLA_{1.7k} or DID/MPEG_{2k}-PDLLA_{4k}-PLL_{1k} via intravenous injection until the tumor diameter was about 8 mm, respectively. Each group had three mice, and the final injected dose of DID in each mouse was 100 µg/kg [65]. The mice were anesthetized by 10% chloral hydrate solution (300 µg/kg, chloral hydrate) before near-infrared imaging at predetermined. The real-time monitoring was detected by a fluorescence imaging system (IVIS Lumina Series III, PerkinElmer, USA; excitation = 645 nm, emission = 715 nm long pass) at the time interval of 2 hrs, 6 hrs and 24 hrs. At the 24 hrs post-injection, the mice were sacrificed, and the heart, liver, spleen, lung, kidney and tumor were harvested to evaluate the *ex vivo* organs' fluorescence intensity. The quantitative fluorescence intensity was acquired using the onboard software.

Anti-tumor effect *in vivo*

The anti-tumor activity of the DTX micelles was investigated in a subcutaneous MCF-7 model and 4T1 model. The process of the subcutaneous tumor model establishment was the same as section tumor targeting of the micelles. The mice were randomized into 5 groups, and injected subcutaneously with 0.1ml of cell suspension containing 1×10^6 cells per mouse. When the tumor diameter was approximately 8 mm, the mice were double-blind randomly divided into control group, free DID group, DID/MPEG_{2k}-PDLLA_{1.7k} group and DID/MPEG_{2k}-PDLLA_{4k}-PLL_{1k} group which were intravenously injected with NS (control), free DTX (dose of DTX: 10 mg/kg), DTX/MPEG_{2k}-PDLLA_{1.7k} (dose of DTX: 10 mg/kg),

DTX/MPEG_{2k}-PDLLA_{4k}-PLL_{1k} (dose of DTX: 10 mg/kg) and blank MPEG-PDLLA-PLL micelles (dose of copolymer: 90 mg/kg) for three consecutive days. Tumor size and body weight were measured every other day during the experimental period and the tumor volumes were calculated from the formula: volume (mm³) = length × width² × 0.5. For MCF-7 model, there were eight mice per group. When the tumor diameter was reached 20 mm, five mice in each group were sacrificed, and the tissues were excised for further analysis. The tumor growth trend would be monitored on the other three mice. For 4T1 model, there were ten mice per group. Five mice in each group were sacrificed until the mice began to die, and the *ex vivo* tissues were harvested for further analysis. The survival time of 4T1 tumor-bearing mice was observed on the other five mice in each group.

To investigate the therapeutic effects further, the apoptosis of the tumor cells was detected by terminal deoxynucleotidyl transferase-mediated nick-end labeling (TUNEL) (TUNEL, Promega, Madison, WI, USA) staining assay, and the proliferation of the tumor cells was analyzed by immune histochemical staining of Ki-67 (Ki-67) (LabVision, MA, USA). On the seventh day after administration, we killed the mice and harvested the tumor tissues. The tumor tissues were fixed in the 15%wt formaldehyde once the mice were killed. The TUNEL method was used according to the manufacturer's instructions and the Ki-67 staining was processed by using the labeled streptavidin-biotin method. The apoptosis and the proliferation of the tumor cells were detected by the fluorescence microscope (Olympus, China).

To investigate the damage caused by DTX formulations *in vivo*, the *ex vivo* normal organs and tumor were obtained. The tissue samples were preserved in 10% buffered formaldehyde for 2 days. The damage of the tissue was visualized by hematoxylin and eosin staining (H&E stain).

Statistical analysis

The comparison of each group was evaluated by the statistical analysis with one-way analysis of variance (ANOVA) using SPSS software. All the data were expressed as the average value ± SD, and a P value <0.05 was considered statistically significant.

Results and Discussion

Characterization of the MPEG-PDLLA-PLL copolymers

MPEG-PDLLA was synthesized by our group through ROP between MPEG and D, L-lactide [42, 53]. MPEG-PDLLA-PLL was synthesized by conjugating PLL with the MPEG-PDLLA. The structures of the

copolymers were characterized by $^1\text{H-NMR}$ and FTIR (figure S1 and figure S2). In figure S1, the characteristic peaks of PLL were h (-CH-, 4.62 ppm), i (-CH₂-, 1.35 ppm), j (-CH₂-, 2.74 ppm), which could be found in the $^1\text{H-NMR}$ spectrum of MPEG-PDLLA-PLL. The molecular weights of the copolymers were calculated using an integral ratio of CH₃O- (a, at 3.33 ppm) to PDLLA and PLL, respectively. The copolymers with different molecular weights are displayed in Table 1. These results indicated that the MPEG-PDLLA-PLL had been synthesized successfully.

Preparation and Optimization of the DTX loaded polymeric micelles

DTX micelles were prepared by thin film hydration method. The properties of DTX micelles, prepared from different molecular weight copolymers, were investigated in detail and the results were listed in Table 1. MPEG was regarded as the most common hydrophilic segments owing to its

biocompatibility and extensive application in pharmaceutical field. Nowadays, due to MPEG with macro molecular weight (over 3.5k Da) might lead to metabolism or other immune-genetic associated problem, PEG_{2k} was extensively used in micelle preparation [66, 67]. Therefore, in this study, the PEG_{2k} as a certain hydrophilic segment to form the shell structure of micelle. Particle size as a basic characteristic of micelles was determined by DLS. From figure 2A, the particle size of MPEG_{2k}-PDLLA_{1.7k}-PLL_{0.5k} could not be determined by its extremely instable, and sizes of the other copolymer micelles were less than 200 nm, which was contributed to concentrate in tumor site through EPR effect (figure 1) [4, 5]. Furthermore, stability and entrapment efficiency of micelles were affected by the drug feeding and molecular weight of copolymer, and they were two important indicators for evaluation of micellar drug loading capacity.

Table 1. The drug loading, entrapment efficiency, stability and sizes of micelles with different block ratio copolymers.

MPEG _x -PDLLA _y -PLL _z	Mw (Da)	Drug Feeding (wt %)	DL (%)	EE (%)	Stability (25 °C)		Size (nm)
					Self-assemble (hr)	Resolved (hr)	
2k-1.7k	3758	5	4.90±0.23	97.91±4.51	4	4	20±2
		8	7.66±0.2	95.97±2.47	1	1	22±3
		12	11.15±0.08	92.88±0.64	0.5	0.5	23±3
2k-1.7k-0.5k	4236	5	4.28±0.46	85.26±7.2	0.5	0.25	*
		10	8.95±0.32	*	*	*	*
2k-4k	6042	5	4.36±0.34	87.20±6.8	0.5	0.25	40±10
		10	9.26±0.41	93.15±7.21	0.5	0.25	*
2k-4k-0.5k	6517	5	4.76±0.26	95.20±5.02	2h	2	42±3
		10	9.51±0.64	93.24±6.23	0.5	0.5	44±5
		20	12.65±1.28	63.25±6.40	0.5	0.25	*
		30	16.24±0.94	54.13±3.13	0.5	0.25	*
2k-4k-1k	7069	5	4.83±0.17	96.64±3.50	24	24	43±2
		10	10.09±0.73	100.25±7.28	12	12	45±3
		20	19.68±0.82	95.53±3.98	4	4	48±5
		30	26.70±1.18	90.18±3.99	1	1	126±4
		40	29.43±6.74	73.51±16.84	1	1	186±50
2k-4k-2k	8071	5	4.85±0.21	97.42±3.78	1	1	104±5
		10	9.78±0.76	97.82±7.58	1	1	110±8
		20	17.49±0.84	90.01±1.64	0.5	0.5	*
		30	21.1±4.42	70.35±14.72	*	*	*
		5	4.77±0.18	95.42±3.58	0.5	0.25	85±6
2k-4k-4k	10112	10	9.37±0.32	93.39±3.51	0.5	0.25	92±5
		20	5.18±0.95	25.78±4.87	*	*	*
		30	3.78±1.23	12.63±4.07	*	*	*
5k-3k-2k	10063	5	4.69±0.24	93.81±0.95	0.5	0.25	49±4
		10	9.21±0.36	90.44±2.02	0.5	0.25	51±3
		20	12.43±2.52	62.89±11.86	*	*	*
		30	14.69±1.17	48.97±3.9	*	*	*

* was indicated the property of micelles could not be determined.

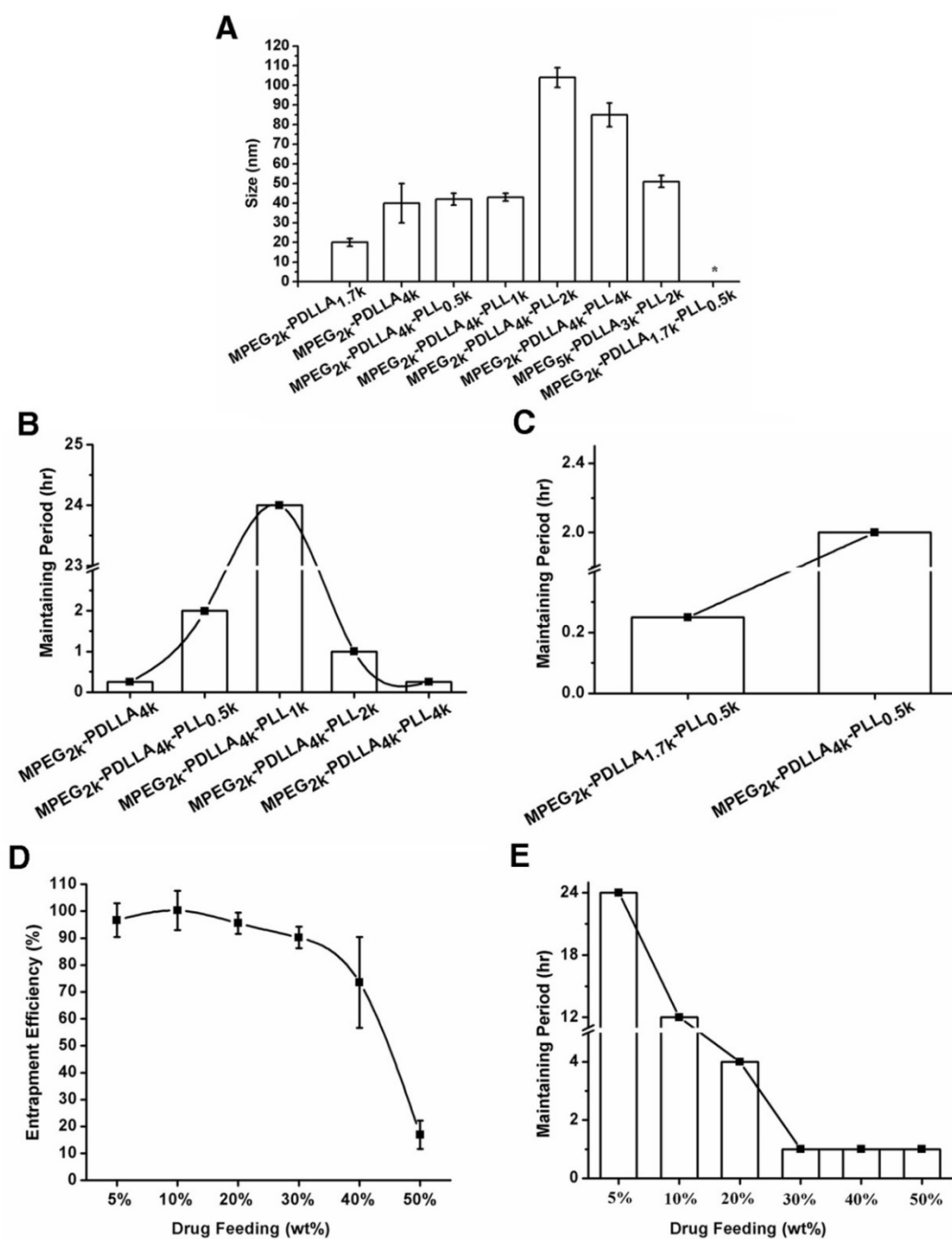


Figure 2. The particle sizes of the DTX loaded micelles (the drug feeding was 5%) based on different molecular weight of copolymers (A); the maintaining period of DTX loaded micelles based on the MPEG_{2k}-PDLLA_{4k}, MPEG_{2k}-PDLLA_{4k}-PLL_{0.5k}, MPEG_{2k}-PDLLA_{4k}-PLL_{1k}, MPEG_{2k}-PDLLA_{4k}-PLL_{2k} and MPEG_{2k}-PDLLA_{4k}-PLL_{4k} (B); the MPEG_{2k}-PDLLA_{1.7k}-PLL_{0.5k} and MPEG_{2k}-PDLLA_{4k}-PLL_{0.5k} (C) with the 5% of drug feeding; the entrapment efficiency change (D) and the maintaining period (E) of DTX/MPEG_{2k}-PDLLA_{4k}-PLL_{1k} micelles with the increased of drug feeding, respectively. ("*") was indicated the particle size of micelle could not be determined.)

We have first investigated the effect of the molecular weight of the hydrophilic and hydrophobic segment in MPEG-PDLLA on the stability of DTX micelles. And the results revealed that the DTX micelles formed by MPEG-PDLLA consist of mPEG_{2k} and PDLL_{1.7k} was more stable than the others. PLL was added to the polymer chain of MPEG_{2k}-PDLLA_{1.7k} to evaluate the effect of PLL segment to the stability of MPEG-PDLLA micelles. The stability of DTX micelles formed by

MPEG_{2k}-PDLLA_{1.7k}-PLL_{0.5k}, however, had been dramatically decreased, as listed in Table 1. It might ascribe to the increase of hydrophilic percentage of the polymer chain. In order to solve the problem, we further increased the molecular weight of PDLLA segments. And the effect of PLL segments on the stability of the DTX micelles formed by MPEG-PDLLA-PLL triblock copolymer was studied in detail and discussed as following:

Effect of PLL's molecular weight on micellar stability

To improve the hydrophilic of the copolymer, PLL was modified to MPEG_{2k}-PDLLA_{4k}. Under the fixed drug feeding and molecular weight of MPEG and PDLLA, we optimized the effect of PLL molecular weight on the stability of DTX micelles and the results were displayed in figure 2B. As the increase of molecular weight of PLL from 0k Da to 1k Da, the maintaining period of DTX/MPEG-PDLLA-PLL was increased from 15 min to 24 hrs. It indicated that the introduction of PLL can affect the stability of DTX/MPEG-PDLLA-PLL micelles. While further increase the PLL molecular weight from 1k Da to 4k Da, however, the maintaining period had decreased from 24 hrs to 30 min. it could conclude that we could obtain the DTX/MPEG_{2k}-PDLLA_{4k}-PLL_{1k} micelles with the longest maintaining period while the molecular weight of PLL was 1k Da. It might be ascribed to the molecular weight of the PLL was above 2k Da, which resulting in the hydrophilicity of the copolymer was too strong to form stable core-shell structure.

Effect of PDLLA's molecular weight on micellar stability

PDLLA was the only hydrophobic segment in this triblock copolymer, which determined the oil-water balance of the copolymer. From figure 2C, it was easy to find that the stability of MPEG_{2k}-PDLLA_{4k}-PLL_{1k} (2 hrs, DL 5%) was superior to MPEG_{2k}-PDLLA_{1.7k}-PLL_{0.5k} (15 min, DL 5%). For the diblock copolymers, however, the maintain period of DTX/MPEG_{2k}-PDLLA_{1.7k} micelles was decreased from 4 hrs to 15 min, while the molecular weight of PDLLA was increased from 1.7k Da to 4k Da. So, when the hydrophilic segment was a certain molecular weight, adjusting the molecular weight of hydrophobic segment was also a way to increase the micellar stability. In this study, in consideration of the investigation on effect of the molecular weight on micellar stability in previous section, PDLLA 4k Da was used as the hydrophobic segment of MPEG-PDLLA-PLL for further exploration.

Effect of drug feeding on the micellar stability

According to the results of the comparison of drug loading capacities of copolymers with different molecular weight, MPEG_{2k}-PDLLA_{4k}-PLL_{4k} micelle was selected for the further investigation. As shown in figure 2E, it was easy to find that the maintaining period has decreased from 24 hrs to 1hr during the drug feeding increased from 5% to 50%. When drug feeding was 20%, however, the maintaining period was 4 hrs, as long as the list DTX formulation

Nanoxel-PM™ (DL was 5%). It indicated that DTX/MPEG_{2k}-PDLLA_{4k}-PLL_{4k} micelle was stable with high drug feeding. Moreover, the EE of the micelle remained above 95% when the drug feeding was increased from 5% to 20% (figure 2D). Hence modifying 1k Da of the PLL onto MPEG_{2k}-PDLLA_{4k} could achieve a high drug loading capacity of DTX micellar carrier. In this study, in consideration of DL and stability, the DTX/MPEG_{2k}-PDLLA_{4k}-PLL_{1k} micelle with 10% DL was used as a novel DTX formulation for exploration in detail.

Characterization of DTX/MPEG_{2k}-PDLLA_{4k}-PLL_{1k} micelle

The critical micelle concentration (CMC) of the MPEG_{2k}-PDLLA_{4k}-PLL_{1k} micelles and MPEG_{2k}-PDLLA_{1.7k} micelles was determined by fluorophotometer (LS55, Perkin Elmer). The CMC of the MPEG_{2k}-PDLLA_{4k}-PLL_{1k} micelles was 10⁻³ mg/ml, as same as the MPEG_{2k}-PDLLA_{4k}-PLL_{1k} micelles (10⁻³ mg/ml), which could remain stable in blood (figure S3).

Morphological study of the DTX/MPEG_{2k}-PDLLA_{4k}-PLL_{1k} was determined by DLS and TEM. The size distribution of the DTX/MPEG_{2k}-PDLLA_{4k}-PLL_{1k} (the DL was 10%) micelles was around 50 nm, which was slightly larger than the blank micelles (48 nm) (figure 3). Moreover, as shown in figure 3A, the particle size did not increase after the DTX/MPEG_{2k}-PDLLA_{4k}-PLL_{1k} micelles were re-dissolved. The result was similar with the formulation which appeared as compact spheres by transmission electron microscopy (figure 3C).

Zeta potential of DTX/MPEG_{2k}-PDLLA_{4k}-PLL_{1k} was around 28±2.14 mV, as shown in figure 3B, lyophilized did not change this property. The positive charges on micelle surface were derived from the amino of PLL.

Crystallographic assay was performed by XRD and the result was shown in Figure S4. In comparison with blank MPEG_{2k}-PDLLA_{4k}-PLL_{1k} and DTX, the graph of DTX/MPEG_{2k}-PDLLA_{4k}-PLL_{1k} lacked the characteristic diffraction peaks, indicating that DTX was completely wrapped in the micelles. These results suggested that the DTX/MPEG_{2k}-PDLLA_{4k}-PLL_{1k} micelles were produced successfully.

Molecular modeling study

In order to further study the mechanism of the copolymer loaded DTX, the dynamics simulation technique was used for simulating its variation of conformations. The 3D structure of the DTX micelles is shown in figure 4. The self-assembly processes of the DTX/MPEG_{2k}-PDLLA_{1.7k} micelles and DTX/MPEG_{2k}-PDLLA_{4k}-PLL_{1k} micelles in annealing

dynamics simulation were presented in figure 5. Initially, the DTX was close to PDLLA, while the hydrophilic segments formed the shell. Then the DTX was entrapped by the polymers. For MPEG_{2k}-PDLLA_{1.7k}, the PDLLA was not long enough to entrap DTX molecules completely, and the DTX molecule was only on the concave zone of the surface of the micellar structure. For MPEG_{2k}-PDLLA_{4k}-PLL_{1k}, however, the molecular weight of PDLLA was 4k Da and the degree of polymerization was 45, which had enough space to touch the DTX. The PLL was one of the hydrophilic segments in MPEG_{2k}-PDLLA_{4k}-PLL_{1k}, which could form the shell structure with MPEG to package DTX molecules completely in the core. It indicated that the molecular structure of MPEG_{2k}-PDLLA_{4k}-PLL_{1k} was definitely conducive for DTX inclusion. In addition, due to the existence of the amino groups on PLL segment (figure 6), a large

number of the hydrogen bonds between DTX and MPEG_{2k}-PDLLA_{4k}-PLL_{1k} promoted the micellar stability. Furthermore, the interactions between copolymers and DTX molecules were investigated and the results were shown in table 2. The $E_{\text{interaction}}$ of DTX/MPEG_{2k}-PDLLA_{4k}-PLL_{1k} micelles (-107.0920 kJ/mol) was lower than $E_{\text{interaction}}$ of DTX/MPEG_{2k}-PDLLA_{1.7k} micelles (-40.9464 kJ/mol), which indicated that the DTX/MPEG_{2k}-PDLLA_{4k}-PLL_{1k} micelles were more stable. Therefore, both the non-bonded interaction and the complete drug cover contributed to the high DL and stability.

Table 2. Interaction Energy and Energies of components contributed to it (kJ/mol)

System	E_{complex}	$E_{\text{copolymer}}$	$E_{\text{docetaxel}}$	$\Delta E_{\text{interaction}}$
DTX/MPEG _{2k} -PDLLA _{1.7k}	-1441.0494	-1356.4659	-43.6371	-40.9464
DTX/MPEG _{2k} -PDLLA _{4k} -PLL _{1k}	-4125.8341	-3975.1050	-43.6371	-107.0920

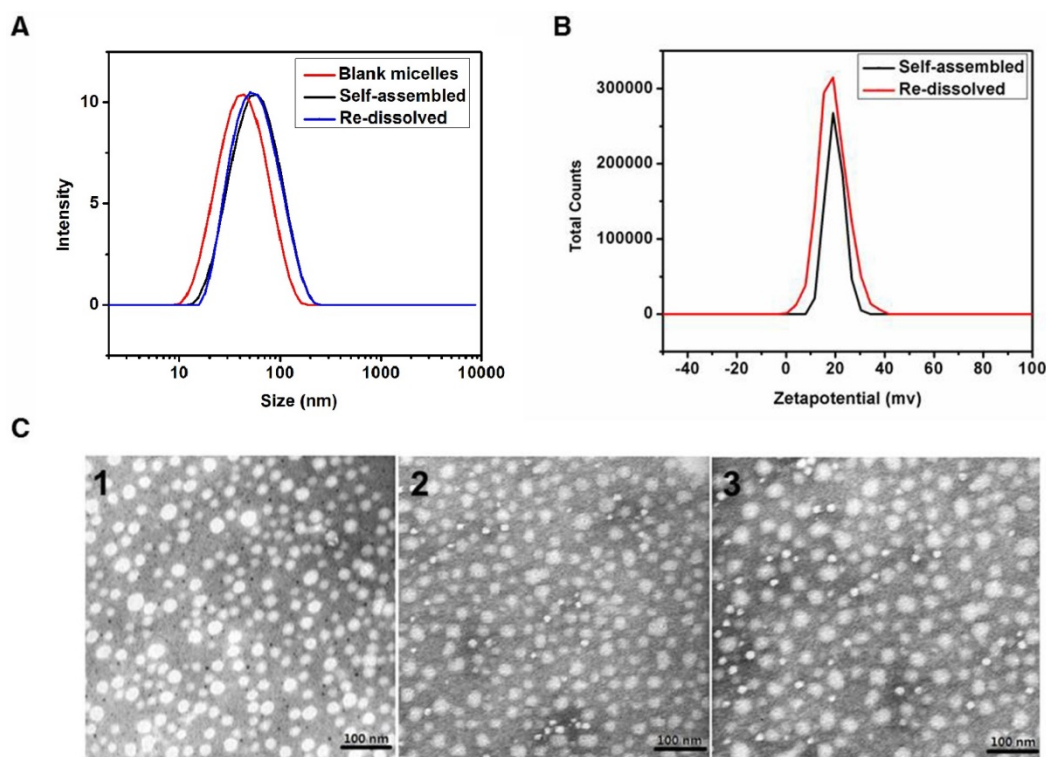


Figure 3. Characterization of DTX/MPEG_{2k}-PDLLA_{4k}-PLL_{1k}. The particle size distribution (A) and zeta potential (B) of the micelles were measured by DLS; TEM images of blank micelles 1, DTX/MPEG_{2k}-PDLLA_{4k}-PLL_{1k} micelles (Self-assembled 2 and Re-dissolved 3) (C).

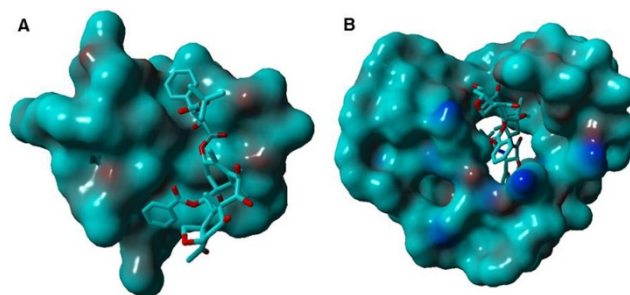


Figure 4. The surface binding state of DTX/MPEG_{2k}-PDLLA_{1.7k} (A), DTX/MPEG_{2k}-PDLLA_{4k}-PLL_{1k} (B), respectively. DTX was represented by the thin stick, the copolymers were depicted with solid surface.

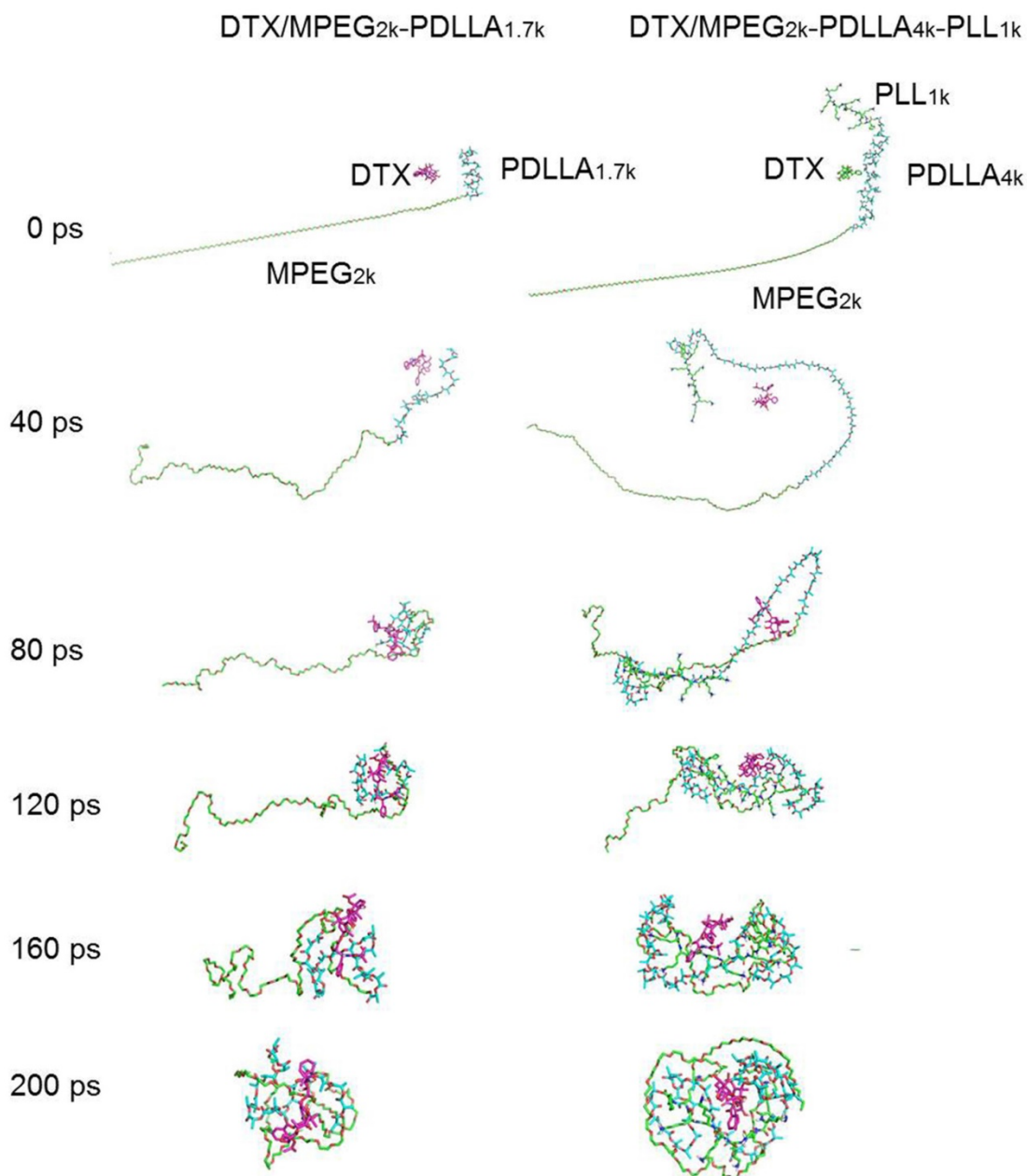


Figure 5. The dynamics simulation annealing process of the DTX/MPEG_{2k}-PDLLA_{1.7k} and DTX/MPEG_{2k}-PDLLA_{4k}-PLL_{1k}, respectively.

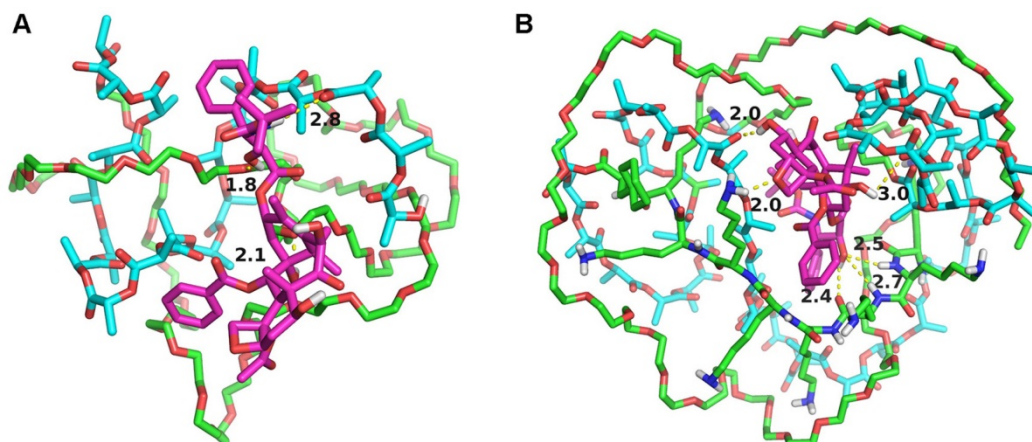


Figure 6. Interaction models between the MPEG_{2k}-PDLLA_{1.7k} (A), MPEG_{2k}-PDLLA_{4k}-PLL_{1k} (B) and DTX. DTX molecule, hydrophobic block and hydrophilic block was represented by the red stick, cyan stick and green stick, respectively. Shot dash line was the hydrogen-bond, the number was length (Å).

The study of drug release behavior *in vitro*

The stability of DTX/MPEG_{2k}-PDLLA_{1.7k} and DTX/MPEG_{2k}-PDLLA_{4k}-PLL_{1k} was quantified by the content of DTX remaining in the micelles aqueous solution. As shown in figure 7A, the DTX content in micelles decreased with the extension of time. At 120 hrs, 74.7% DTX leaked from the MPEG_{2k}-PDLLA_{1.7k} micelles, and 25.2% DTX leaked from the MPEG_{2k}-PDLLA_{4k}-PLL_{1k} micelles. It indicated that the stability of DTX/MPEG_{2k}-PDLLA_{4k}-PLL_{1k} micelles in pH7.4 PBS solution was superior to DTX/MPEG_{2k}-PDLLA_{1.7k} that of micelles.

The *in vitro* release behavior of free DTX and DTX micelles based on MPEG_{2k}-PDLLA_{1.7k} and MPEG_{2k}-PDLLA_{4k}-PLL_{1k} are shown in figure 7B. In the free DTX group, 94.9% DTX was released into the media within 24 hrs, and the micelle groups released 73.8% and 56.2%, respectively. It suggested that the micelles could prevent drug release quickly. Similarly, 96.6% of DTX was released from the

MPEG_{2k}-PDLLA_{1.7k} micelles, while 76.4% of DTX was released from the MPEG_{2k}-PDLLA_{4k}-PLL_{1k} micelles within 120 hrs. So the DTX/MPEG_{2k}-PDLLA_{4k}-PLL_{1k} micelles could provide extended sustained release of DTX, compared with the behavior of DTX/MPEG_{2k}-PDLLA_{1.7k} micelles.

Furthermore, the drug release behavior of the DTX/MPEG_{2k}-PDLLA_{4k}-PLL_{1k} micelles in different pH media was investigated, and the results were exhibited in figure 7C. In the first 12 hrs, 80% of DTX was released in the acid medium; only 40% of DTX was released in the basic medium. Finally, the drug was released completely in the medium with pH5. Therefore, MPEG_{2k}-PDLLA_{4k}-PLL_{1k} might prevent drug release in the basic environment while promoting drug release in the acidic environment, and the mechanism of this phenomenal would be researched in detail in the future. This property of DTX/MPEG_{2k}-PDLLA_{4k}-PLL_{1k} might enable the specific release of DTX at the acidic tumor site.

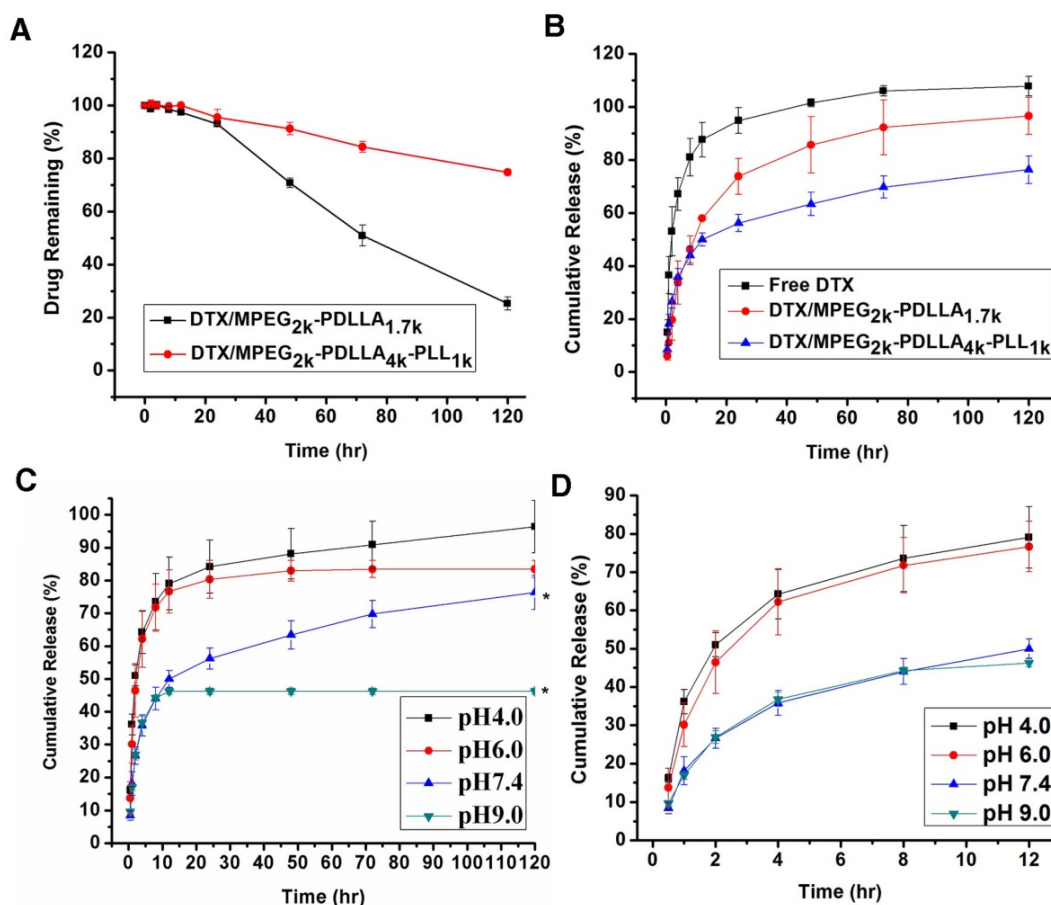


Figure 7. The release profile of DTX formulations. The content of DTX remaining in the micelles aqueous solution (A); the DTX formulations release profiles in PBS 7.4 (B); *In vitro* release profiles of DTX from DTX/MPEG_{2k}-PDLLA_{4k}-PLL_{1k} system in different pH media (C); the first 12 hrs of the *in vitro* release profiles in different pH media (D). Statistical difference from the free DTX group (***) p<0.05)

Hemolysis test and biocompatibility evaluation of the micelles

Since the cationic polymer easily caused hemolysis, the hemolytic test of the MPEG_{2k}-PDLLA_{4k}-PLL_{1k} micelles should be carried out. From figure S5, the hemolysis did not happen at any concentration of MPEG_{2k}-PDLLA_{4k}-PLL_{1k} micelles. The hemolytic rate (0 to 3.10%) of MPEG_{2k}-PDLLA_{4k}-PLL_{1k}, shown in table S1, was under the international standard (5%), which did not cause hemolysis. To trace toxicity caused by the formulations accurately, the normal organs in each group were checked. From figure S7 and S8, no obvious damage appeared in the each group. These results indicated that the DTX/MPEG_{2k}-

PDLLA_{4k}-PLL_{1k} micelles were safe for using in breast cancer therapy.

Delivery of the micelles *in vitro*

To investigate the transport ability of DTX/MPEG_{2k}-PDLLA_{4k}-PLL_{1k} *in vitro*, the fluorescence microscope and flow cytometry were used to analyze the cellular uptake. In this study, C6 was used as a fluorescence indicator to be loaded into the micelles. From figure 8A and B, the fluorescence of the C6 can be observed in the cytoplasm, which indicated that both MPEG_{2k}-PDLLA_{1.7k} and MPEG_{2k}-PDLLA_{4k}-PLL_{1k} could transfer drugs into tumor cells.

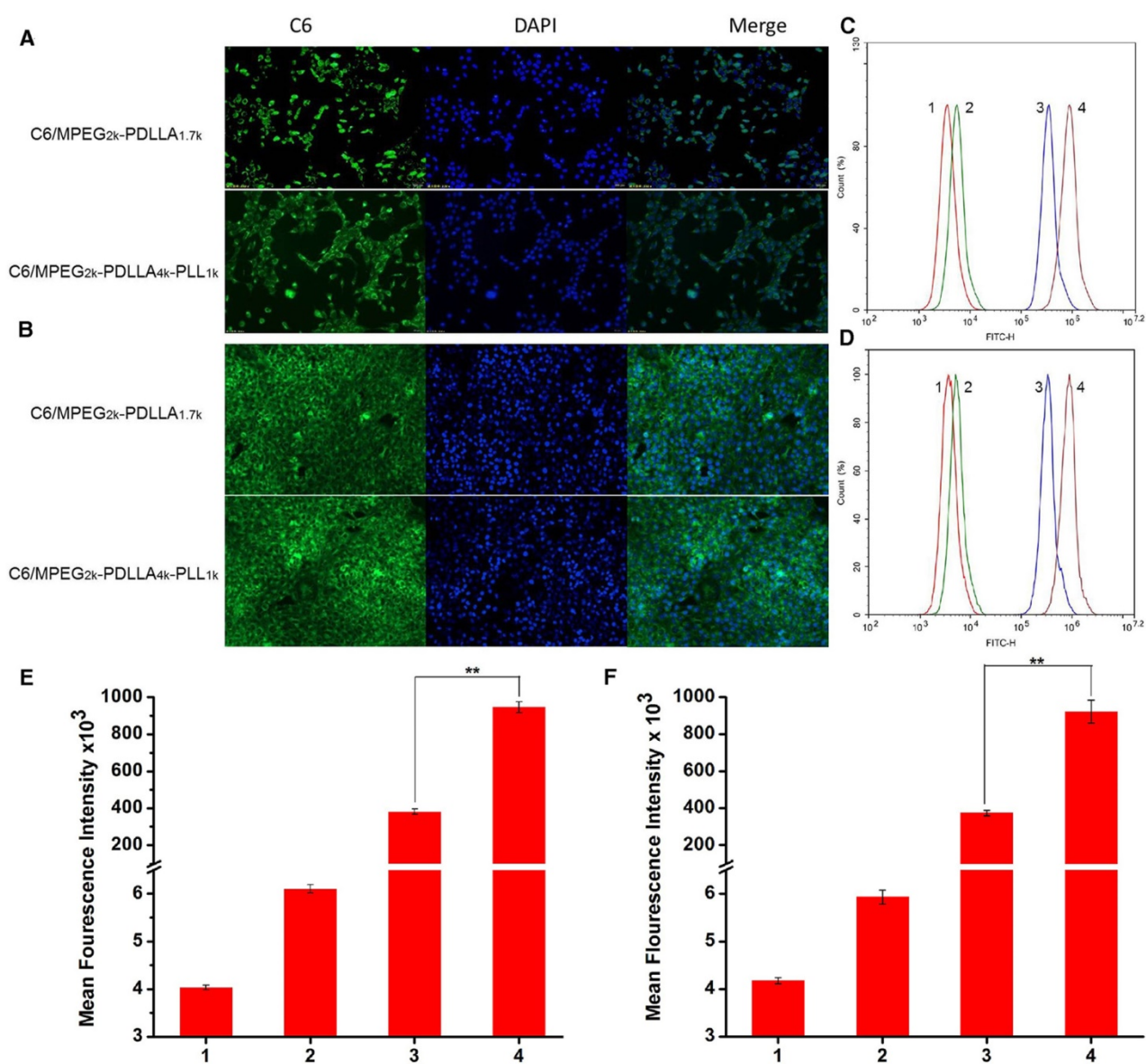


Figure 8. The cellular uptake of micelles. The fluorescence images of micelles by MCF-7 cell lines (A) and 4T1 cell lines (B); Flow cytometer analysis of C6 cellular binding in the MCF-7 cells(C) and 4T1 cells (D), respectively. The quantitative analysis of C6 cellular binding in the MCF-7 cells (E) and 4T1 cells (F), respective. 1, 2, 3, 4 represented control, free C6, C6/MPEG_{2k}-PDLLA_{1.7k} and C6/MPEG_{2k}-PDLLA_{4k}-PLL_{1k}, respectively. Statistical difference between the groups (***) p<0.01)

Furthermore, to quantify the cellular uptake of the DTX micelles, the intensity of the tumor cells, treated with different formulations, was detected by flow cytometer, and the results are shown in figure 8C and D, respectively. The fluorescence signal of the free C6 group was stronger than the control group, but much weaker than the micelle groups. Moreover, as shown in figure 8E and F, the fluorescence signal intensity of the C6/MPEG_{2k}-PDLLA_{4k}-PLL_{1k} group was three times that of the C6/MPEG_{2k}-PDLLA_{1.7k} group. In 4T1 cell lines, the fluorescence intensity of the C6/MPEG_{2k}-PDLLA_{4k}-PLL_{1k} group and the C6/MPEG_{2k}-PDLLA_{1.7k} group was consistent with that of MCF-7 cells. Therefore, these results indicated that the micelles would be an effective way to promote cell uptake for hydrophobic drugs, and MPEG_{2k}-PDLLA_{4k}-PLL_{1k} was suitable to cargo hydrophobic drugs into cells.

In vitro cytotoxicity of the micelles

The MTT assay and the apoptosis experiments were used to evaluate cytotoxicity of DTX formulations. The results of MTT assay on HEK293 cells and HUVEC cells (figure S6) indicated that low toxicity of the MPEG_{2k}-PDLLA_{4k}-PLL_{1k} micelles for normal cells. From figure 9A and 9B, it can be seen that all the DTX formulations can inhibit the growth

of 4T1 cells and MCF-7 cells in a dose-dependent manner, and the blank MPEG-PDLLA-PLL micelles were little toxicity for the tumor cells. Moreover, the half maximal inhibitory concentration (IC₅₀) values (figure 9C) of the DTX/MPEG_{2k}-PDLLA_{4k}-PLL_{1k} group on MCF-7 (7.16 μg/ml) and 4T1 (6.35 μg/ml) were much lower than the other groups. Additionally, cell apoptosis experiments were used for MTT assay further certification. The proportion of apoptotic cells in each group was shown in figure 9D. The MCF-7 cell and 4T1 cell apoptosis rate of the DTX/MPEG_{2k}-PDLLA_{4k}-PLL_{1k} group was 45% and 41%, respectively, much higher than the other groups. The results of the cell apoptosis experiments were consistent with the MTT assays. In previous research, micelles were proved to prevent the drug efflux mediated by P-glycoproteins [68]. So compared with free DTX, the cellular uptake enhancement and intracellular retention prolongation of DTX-loaded micelles improved the cytotoxicity for tumor cells. Also, the anti-tumor effect of DTX/MPEG_{2k}-PDLLA_{4k}-PLL_{1k} was superior to DTX/MPEG_{2k}-PDLLA_{1.7k} micelles, which would contribute to the stability and the micellar affinity of the MPEG_{2k}-PDLLA_{4k}-PLL_{1k} micelles to cells [50].

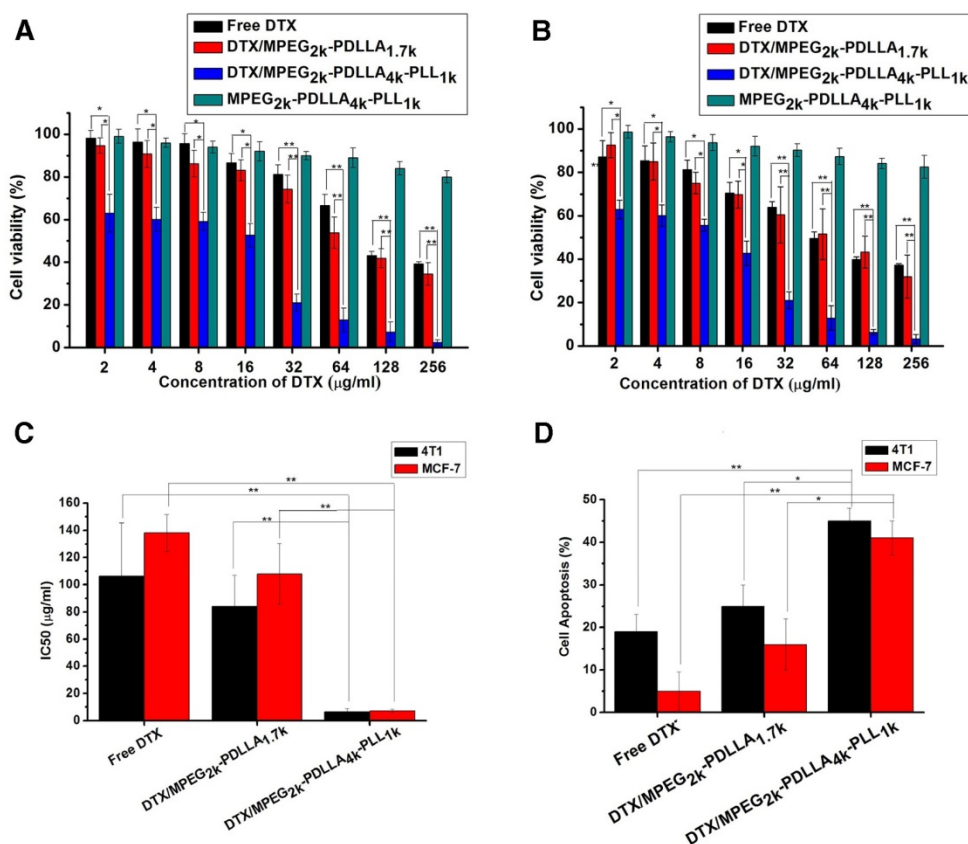


Figure 9. The anti-tumor effect of the DTX formulations. Cytotoxicity studies on 4T1 cells (A) and MCF-7 cells (B); C: IC₅₀ value of DTX formulations on 4T1 and MCF-7 cells; D: Cell apoptosis on 4T1 and MCF-7 cells; Statistical difference from the free DTX group (***) p<0.05 (***) p<0.01)

Delivery of the micelles *in vivo*

The *in vivo* targeting ability of MPEG_{2k}-PDLLA_{4k}-PLL_{1k} micelles for a MCF-7 cells tumor engraftment was investigated on nude mice. DID was used as the fluorescent chromogenic agent entrapped in micelles for the real-time drug delivery efficiency test by fluorescence imaging system. During 2 hrs post-injection the same dose of DID, the fluorescence images of tumors was presented in figure 10A, the tumor fluorescence signals of mice treated with DID micelles were significantly stronger than that treated with free DID, and DID fluorescence of the micelle groups began to concentrate in tumor. As the time was prolonged, the accumulation of fluorescent signals in tumors reached the peak levels at 6 hrs. The tumor fluorescence intensity of the DID/MPEG_{2k}-

PDLLA_{4k}-PLL_{1k} group was much higher than that the DID/MPEG_{2k}-PDLLA_{1.7k} group. At 24 hrs post-injection, the fluorescent signals in mice were decreased. Furthermore, to evaluate the biodistribution in mean organs, the mice were sacrificed, and fluorescent signals in *ex vivo* mean organs and tumors were determined (figure 10B). The fluorescence intensity of micelle groups was stronger in tumor and weaker in normal organs than the free DID group. Compare with DID/MPEG_{2k}-PDLLA_{1.7k} group, the fluorescence intensity of DID/MPEG_{2k}-PDLLA_{4k}-PLL_{1k} group in tumor was stronger, which was much weaker in heart, kidney and lung. These results indicated that drugs could be accumulated into tumor sites through MPEG_{2k}-PDLLA_{4k}-PLL_{1k}.

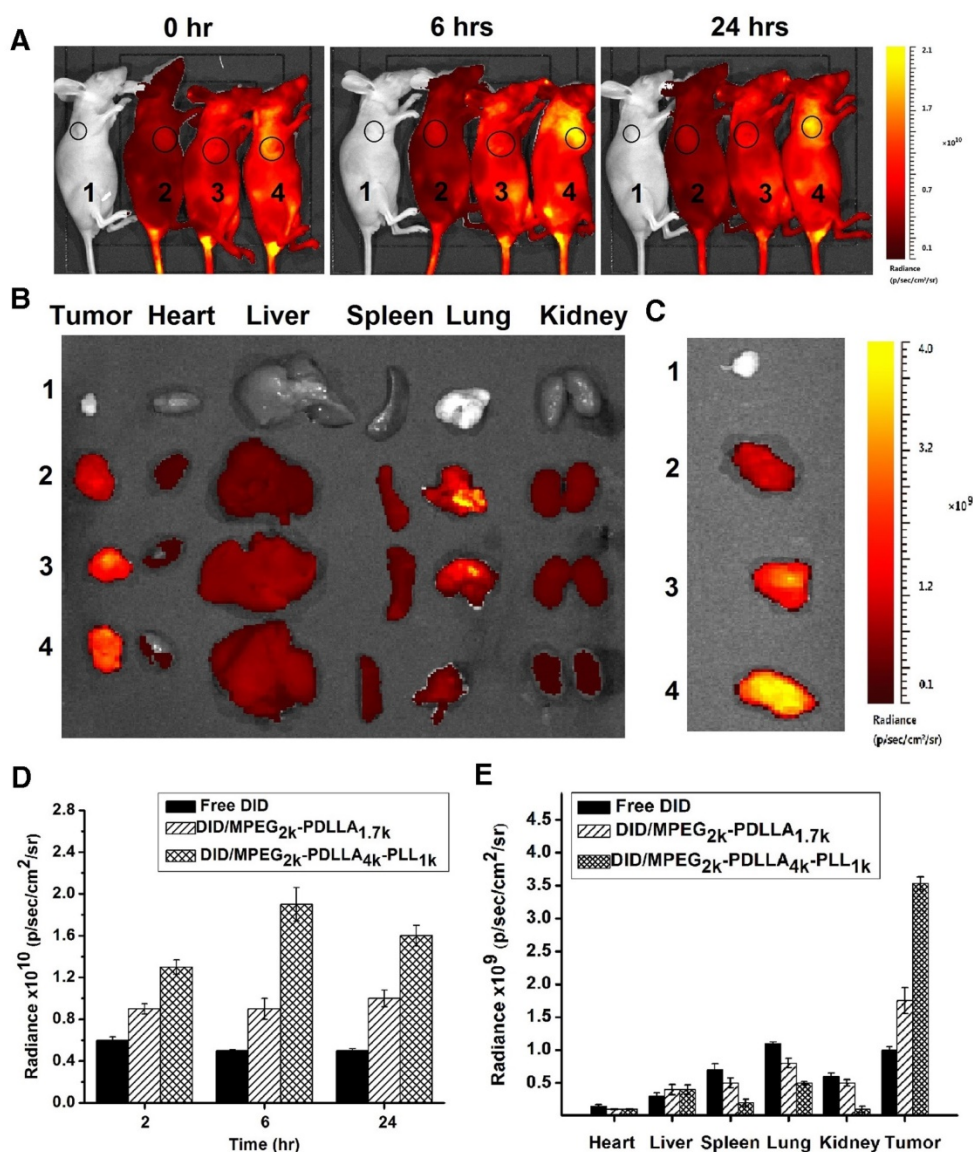


Figure 10. *In vivo* biodistribution of control 1, free DID 2, DID/MPEG_{2k}-PDLLA_{1.7k} 3 and DID/MPEG_{2k}-PDLLA_{4k}-PLL_{1k} 4. Real-time fluorescence images of the tumor-bearing mice after intravenous injection at set time points (A); the fluorescence images of *ex vivo* mean organs and tumors at 24 hrs post-injection (B); the fluorescence images of tumors (C); the quantitative analysis of fluorescence intensity in tumors at set time points post-injection (D); the quantitative analysis of fluorescence intensity in *ex vivo* mean organs and tumors (E)

This experimental phenomenon was dependent on the enhancement of micelle-mediated drug delivery efficiency, which was due to the long circulation time caused by surface PEGylation, the ideal particle size and the cell affinity. The PEG molecule on the surface of the micelles could prevent the reticuloendothelial system (RES) recognition and reduce the liver and spleen uptake, endowing the micelles with a longer circulation time [69]. The particle sizes (less than 200 nm) could effectively target the tumor using size-dependent properties and EPR effect of the tumor (figure 1) [4, 5]. Positive ion on the surface of the MPEG_{2k}-PDLLA_{4k}-PLL_{1k} easily promoted the micelles' penetration of the cytomembrane. Therefore, the MPEG_{2k}-PDLLA_{4k}-PLL_{1k} micelles were concentrated in the tumor tissue.

Antitumor activity of micelles *in vivo*

To evaluate the *in vivo* anti-tumor active of DTX/MPEG_{2k}-PDLLA_{4k}-PLL_{1k}, MCF-7 tumor-bearing mice and 4T1 tumor-bearing mice were treated with different DTX formulations, respectively. Because of the weak anti-tumor activity of the blank MPEG_{2k}-PDLLA_{4k}-PLL_{1k} micelles, the results of the evaluation of anti-tumor activity of which were not shown in this section. According to images of MCF-7 tumor bearing mice with different treatments on 28 days after administration (figure 11A), photographs of MCF-7 tumors (figure 11B) and the MCF-7 tumor growth curve (figure 11C), DTX/MPEG_{2k}-PDLLA_{4k}-PLL_{1k} micelles exhibited the most efficient inhibition to proliferation of MCF-7 tumor, and one of the solid tumors in DTX/MPEG_{2k}-PDLLA_{4k}-PLL_{1k} group was removed completely. The tumor volume of DTX/MPEG_{2k}-PDLLA_{1.7k} group was smaller than that of the free DTX group ($p < 0.05$). We have monitored the tumor growth of DTX/MPEG_{2k}-PDLLA_{4k}-PLL_{1k} group for 45 days, and the tumor start to grow at 38 days. In order to further investigate the *in vivo* antitumor effect of DTX formulations, TUNEL staining and Ki-67 staining were used for detecting the MCF-7 tumor cellular apoptosis and proliferation, respectively, and the results were shown in figure 13A and B. The number of the apoptotic bodies in the DTX/MPEG_{2k}-PDLLA_{4k}-PLL_{1k} group was 9.28% (figure 13D), which was higher than the other groups. Furthermore, the activities of different DTX formulations on proliferation of tumor cells were analyzed by Ki-67 (figure 13C). Compared with DTX/MPEG_{2k}-PDLLA_{1.7k} group (60.12%), Free DTX group (67.27%) and control group (78.96%), the Ki67 positive cells in DTX/MPEG_{2k}-PDLLA_{4k}-PLL_{1k} group (31.46%) were a significant decrease. The H&E stain of tumor tissues in different groups were shown in

figure (figure 13E). The most serious damage was observed in DTX/MPEG_{2k}-PDLLA_{4k}-PLL_{1k} group. The results suggested that DTX/MPEG_{2k}-PDLLA_{4k}-PLL_{1k} micelles could inhibit growth of the MCF-7 tumor effectively *in vivo*.

In order to explore the *in vivo* effectiveness of the DTX formulation on different kinds of breast cancer tumors, the tumor growth curve and survival time of the 4T1 tumor-bearing mice was recorded in figure 12C and D, respectively. From the 4T1 tumor growth curve, all DTX formulations showed efficient antitumor ability. DTX/MPEG_{2k}-PDLLA_{4k}-PLL_{1k} micelles could significantly inhibit 4T1 tumor growth ($p < 0.01$), and the antitumor effect could be intuitive in figure 12A and B, which was consistent with the results of the MCF-7 tumor-bearing mice model. Survival time of the 4T1 tumor-bearing mice (figure 12D) was observed for 35 days after administration. Mice in the control group treated with NS were begun to die at 21 days after administration, and the remaining mice were dead within 28 days. Compared to the control group, DTX/MPEG_{2k}-PDLLA_{1.7k} and free DTX could extend the survival time of the 4T1 tumor-bearing mice, but all the mice were dead after 30 days. In contrast, 60% of mice in the DTX/MPEG_{2k}-PDLLA_{4k}-PLL_{1k} group were still alive at 35 days. The TUNEL, Ki67 and H&E stain were furthermore to evaluate the inhibition of 4T1 cell *in vivo*. As shown in figure 14A and 14B, compared with control group, free DTX group and the DTX/MPEG_{2k}-PDLLA_{1.7k} group, weak Ki-67 positive immune-active and the most number of apoptotic cells were observed in DTX/MPEG_{2k}-PDLLA_{4k}-PLL_{1k} group. The damage of tumor tissue was investigated by H&E stain (figure 14E). The intact nucleus number of tumor tissues in DTX/MPEG_{2k}-PDLLA_{4k}-PLL_{1k} group was decreased with the comparison of control group, free DTX and DTX/MPEG_{2k}-PDLLA_{1.7k} group.

It could be found that, both MCF-7 tumors and 4T1 tumors, whose growth could be inhibited by a DTX formulation, and DTX/MPEG_{2k}-PDLLA_{4k}-PLL_{1k} micelles exhibited the maximal anti-tumor active *in vivo*. Therefore, improving the drug loading capacity of micelles could enhance the anti-tumor effect of DTX.

Body weight change rate of the MCF-7 tumor-bearing mice and 4T1 tumor-bearing mice are shown in figure 11D and 12E, respectively. Both in MCF-7 tumor-bearing mice and 4T1 tumor-bearing mice models, the body weights decreased after treatment with the DTX formulation. From the result of *in vivo* bio-distribution, the formulation could not be metabolized completely in normal organs. Therefore, the DTX was accumulated in normal organs after three consecutive days' administration,

which might lead the body weight reduction. The DTX/MPEG_{2k}-PDLLA_{4k}-PLL_{1k} group and DTX/MPEG_{2k}-PDLLA_{1.7k} group had less body weight reduction than the free DTX group, which indicated that the systemic toxicity of the DTX was decreased by loading DTX in micelles. Finally, the body weight of the mice in each group recovered to normal.

Conclusion

In this study, we designed and synthesized the copolymer MPEG_{2k}-PDLLA_{4k}-PLL_{1k} for DTX loading. The MPEG_{2k}-PDLLA_{4k}-PLL_{1k} had a high drug loading capacity. By 3D molecular simulation results of DTX micelles, it revealed that DTX could be completely wrapped in the polymer (MPEG_{2k}-PDLLA_{4k}-PLL_{1k}), which was shown to be embedded in the copolymer (MPEG_{2k}-PDLLA_{1.7k}) surface only. The number of hydrogen bonds between DTX and copolymer molecules in DTX/MPEG_{2k}-PDLLA_{4k}-PLL_{1k} was more

than that in DTX/MPEG_{2k}-PDLLA_{1.7k}. The simulation results supported the high drug loading capacity of MPEG_{2k}-PDLLA_{4k}-PLL_{1k} micelles. The drug release behavior of DTX micelles confirmed the sustained release property of the DTX/MPEG_{2k}-PDLLA_{4k}-PLL_{1k}. By evaluating the cellular uptake and anticancer properties of DTX/MPEG_{2k}-PDLLA_{4k}-PLL_{1k} *in vitro*, it demonstrated that the DTX/MPEG_{2k}-PDLLA_{4k}-PLL_{1k} micelles maintained better anticancer performance than that of DTX/MPEG_{2k}-PDLLA_{1.7k}. The *in vivo* biodistribution image results of the DTX micelles further suggested the tumor targeting effect of the DTX/MPEG_{2k}-PDLLA_{4k}-PLL_{1k}. The good biocompatibility of the DTX/MPEG_{2k}-PDLLA_{4k}-PLL_{1k} was exhibited in a safety evaluation, and the *in vivo* anti-tumor study showed obvious effects in the treatment of breast cancer. In conclusion, DTX/MPEG_{2k}-PDLLA_{4k}-PLL_{1k} would be a promising candidate for breast cancer targeted therapy.

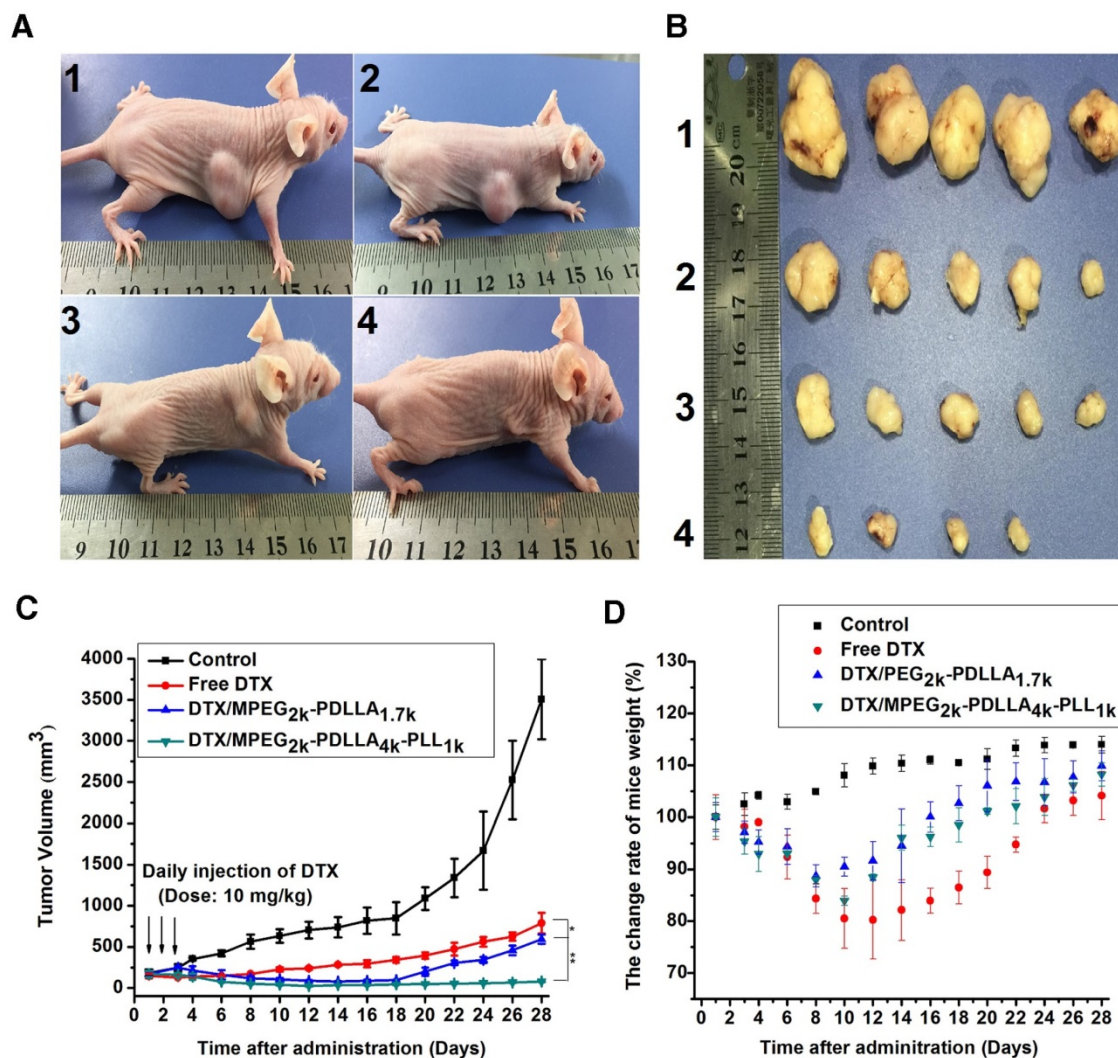


Figure 11. The micelles inhibited tumors growth in MCF-7 model, control 1, free DTX 2, DTX/MPEG_{2k}-PDLLA_{1.7k} 3 and DTX/MPEG_{2k}-PDLLA_{4k}-PLL_{1k} 4. Images of MCF-7 tumor bearing mice with different treatments on 28 days after administration (A); images of subcutaneous tumors in each group (B); growth curves of tumor in the mice (C); body weight of the mice in each group (D). Statistical difference from the free DTX group (***) p<0.05

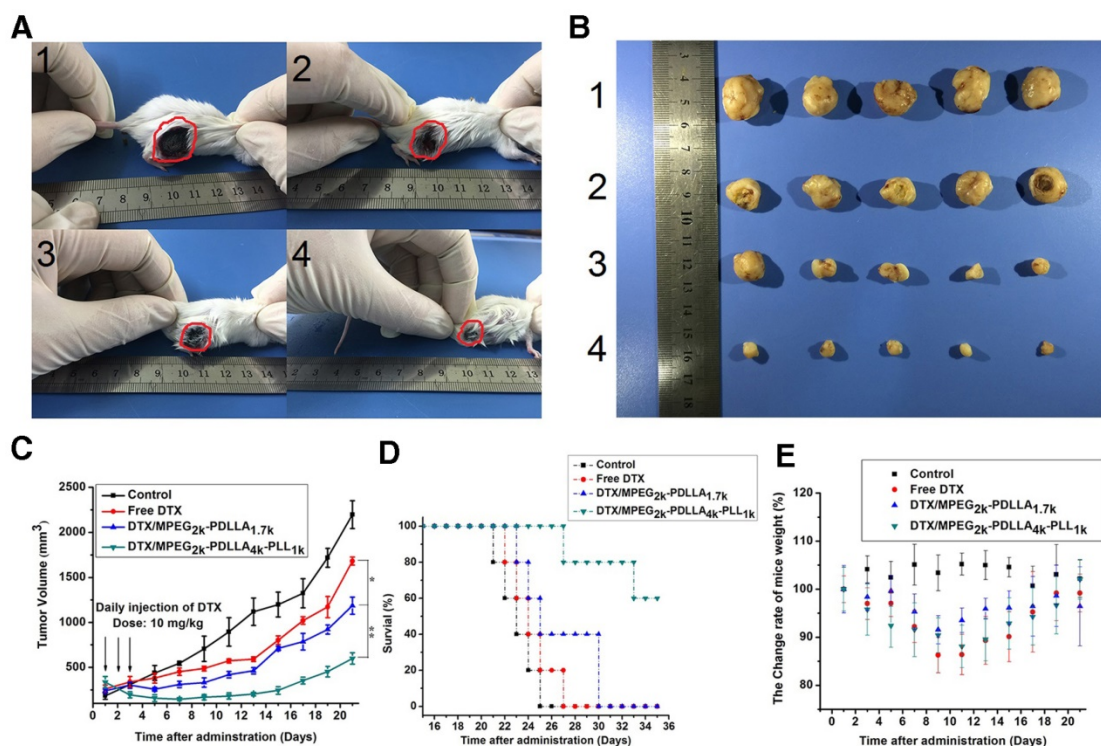


Figure 12. The micelles inhibited tumors growth in MCF-7 model, control 1, free DTX 2, DTX/MPEG_{2k}-PDLLA_{1.7k} 3 and DTX/MPEG_{2k}-PDLLA_{4k}-PLL_{1k} 4. Images of MCF-7 tumor bearing mice with different treatments on 21 days after administration (A); images of subcutaneous tumors in each group (B); growth curves of tumor in the mice (C); Survival of the 4T1 tumor-bearing mice (D); body weight of the mice in each group (E). Statistical difference between groups (***) p<0.05 (****) p<0.01)

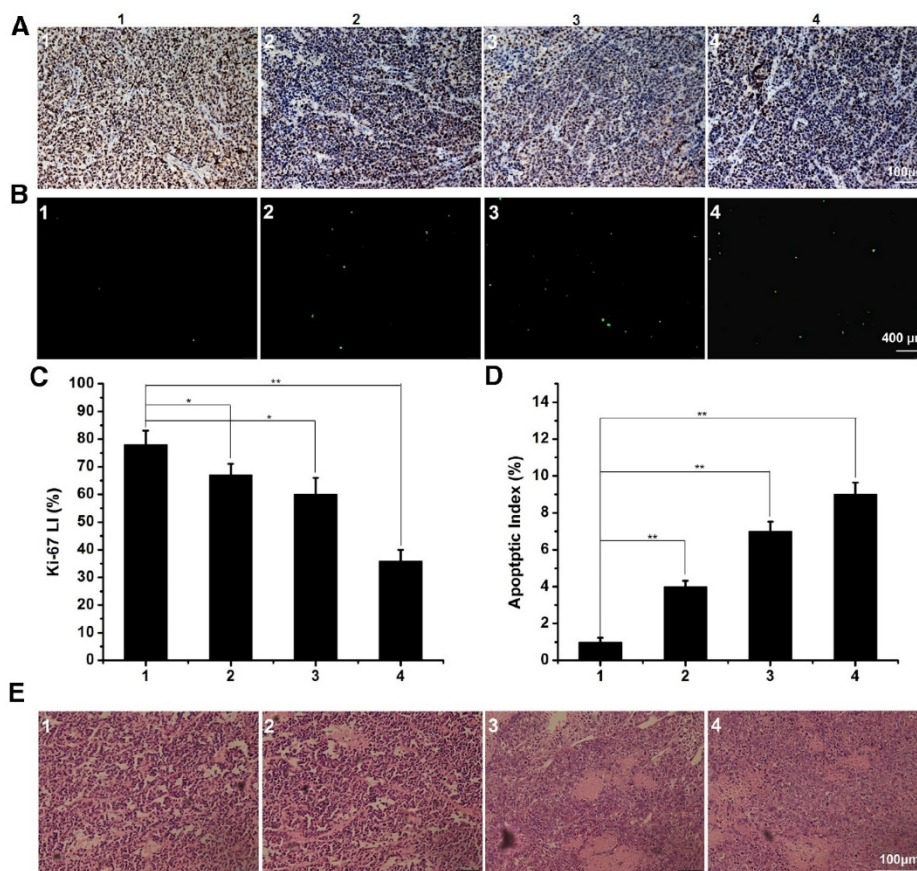


Figure 13. The immunofluorescence staining of tumor slices with treatment of control 1, free DTX 2, DTX/MPEG_{2k}-PDLLA_{1.7k} 3 and DTX/MPEG_{2k}-PDLLA_{4k}-PLL_{1k} 4 in MCF-7 model. A, B and E was representative Ki-67 immunohistochemical, TUNEL immunofluorescent and H&E stain in each group. C and D was the quantitative analysis of Ki-67 immunohistochemical, TUNEL immunofluorescent in each group, respectively. Statistical difference between groups (***) p<0.05 (****) p<0.01).

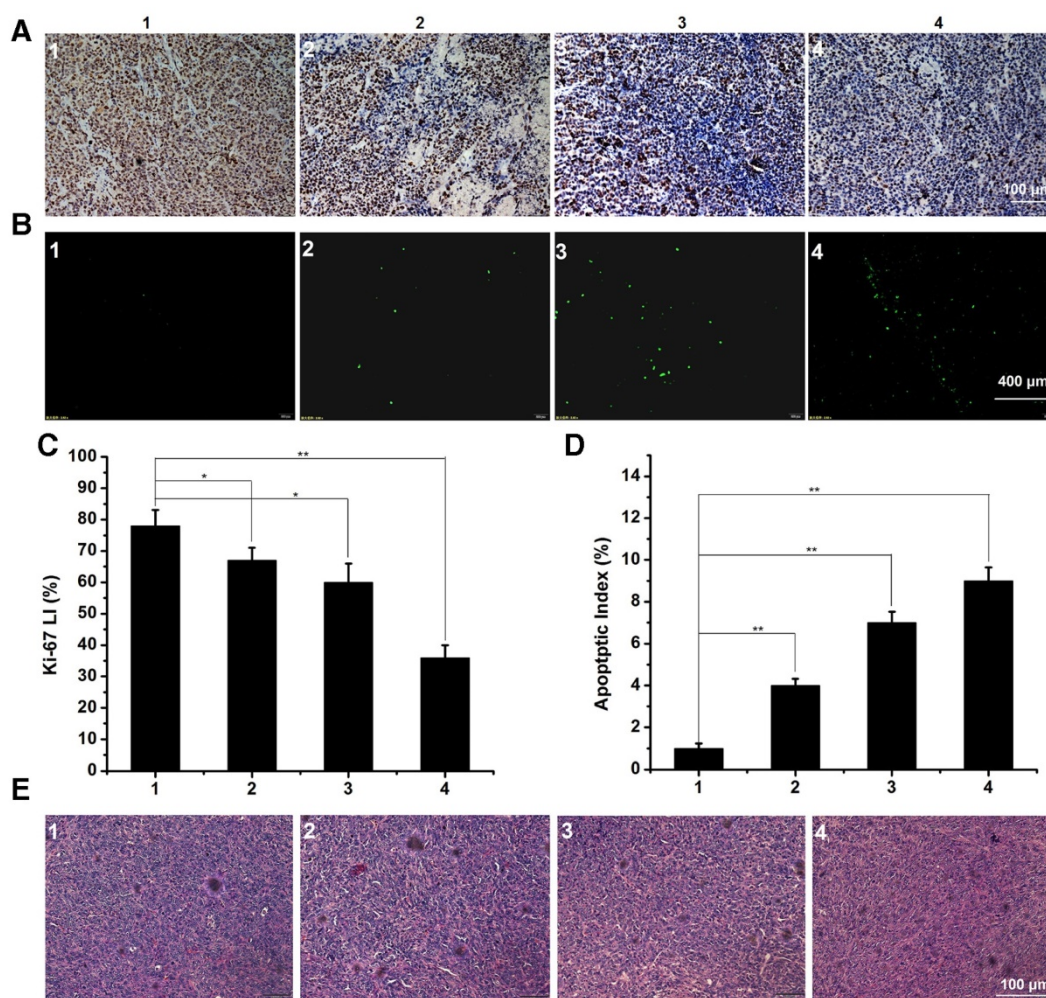


Figure 14. The immunofluorescence staining of tumor slices with treatment of control 1, free DTX 2, DTX/MPEG_{2k}-PDLLA_{1.7k} 3 and DTX/MPEG_{2k}-PDLLA_{4k}-PLL_{1k} 4 in 4T1 model. A, B and E was representative Ki-67 immunohistochemical, TUNEL immunofluorescent and H&E stain in each group. C and D was the quantitative analysis of Ki-67 immunohistochemical, TUNEL immunofluorescent in each group, respectively. Statistical difference between groups (***) $p < 0.05$ (****) $p < 0.01$.

Abbreviations

PLL: Poly (L-Lysine)
 MPEG-PDLLA: Monomethoxy poly (ethylene glycol)-poly (D, L-lactide)
 DTX: Docetaxel
 DL: Drug loading
 EE: Entrapment efficiency
 DTX/MPEG_{2k}-PDLLA_{4k}-PLL_{1k}: DTX loaded MPEG_{2k}-PDLLA_{4k}-PLL_{1k}
 DTX/MPEG-PDLLA: DTX loaded MPEG-PDLLA
 EPR effect: Enhanced permeability and retention effect
 TPGS: D- α -tocopheryl polyethylene glycol 1000 succinate
 RME: Receptor-mediated endocytosis
 Lys (Z)-NCA: N-carboxyanhydride of 6-(benzyloxycarbonyl)-L-lysine
 H-Lys (Z)-OH: N^ε-carboxybenzoxy-L-lysine
 Boc-L-Phe: N-t-butoxycarbonyl-L-phenylalanine
 DiD: 1'-dioctadecyl-3, 3', 3'-tetramethylindotricar-

bocyanine

THF: Tetrahydrofuran;
 FTIR: Fourier Transform Infrared
 ROP: Ring opening polymerization
¹H-NMR: Nuclear magnetic resonance spectroscopy
 GPC: Gel Permeation Chromatography
 DLS: Dynamic light scattering
 TEM: Transmission electron microscopy
 XRD: X-ray diffractometer
 CMC: Critical micelle concentration
 IC₅₀ value: Half maximal inhibitory concentration
 RES: Reticuloendothelial system
 HPLC: High Performance Liquid Chromatography
 MD: Molecular dynamic
 NPT: Equilibrium molecular dynamics simulation of isothermal-isobaric ensemble
 TUNEL: Terminal deoxynucleotidyl transferase-mediated nick-end labeling
 Ki67: Rat antimouse monoclonal antibody
 H&E stain: Hematoxylin-eosin staining

Acknowledgements

This work was financially supported by the National Natural Science Foundation of China (31525009 and 31222023), the National Key Research and Development Program of China (2017YFC1103502), Sichuan Innovative Research Team Program for Young Scientists (2016TD0004), and Distinguished Young Scholars of Sichuan University (2011SCU04B18).

Supplementary Material

Supplementary figures and tables.

<http://www.thno.org/v07p2652s1.pdf>

Competing Interests

The authors have declared that no competing interest exists.

References

- Tyler B, Gullotti D, Mangraviti A, Utsuki T, Brem H. Poly(lactic acid) (PLA) controlled delivery carriers for biomedical applications. *Adv Drug Deliv Rev.* 2016; 107: 163-75.
- Zhou WS, Li CB, Wang ZY, Zhang WL, Liu JP. Factors affecting the stability of drug-loaded polymeric micelles and strategies for improvement. *J Nanopart Res.* 2016; 18: 1-18.
- Gothwal A, Khan I, Gupta U. Polymeric Micelles: Recent advancements in the delivery of anticancer drugs. *Pharm Res.* 2016; 33: 18-39.
- Gong C, Deng S, Wu Q, Xiang M, Wei X, Li L, et al. Improving antiangiogenesis and anti-tumor activity of curcumin by biodegradable polymeric micelles. *Biomaterials.* 2013; 34: 1413-32.
- Wang H, Zhao Y, Wu Y, Hu YL, Nan K, Nie G, et al. Enhanced anti-tumor efficacy by co-delivery of doxorubicin and paclitaxel with amphiphilic methoxy PEG-PLGA copolymer nanoparticles. *Biomaterials.* 2011; 32: 8281-90.
- Deng C, Jiang YJ, Cheng R, Meng FH, Zhong ZY. Biodegradable polymeric micelles for targeted and controlled anticancer drug delivery: Promises, progress and prospects. *Nano Today.* 2012; 7: 467-80.
- Valle JW, Armstrong A, Newman C, Alakhov V, Pietrzynski G, Brewer J, et al. A phase 2 study of SP1049C, doxorubicin in P-glycoprotein-targeting pluronics, in patients with advanced adenocarcinoma of the esophagus and gastroesophageal junction. *Invest New Drugs.* 2011; 29: 1029-37.
- Sanna V, Siddiqui IA, Sechi M, Mukhtar H. Nanoformulation of natural products for prevention and therapy of prostate cancer. *Cancer Lett.* 2013; 334: 142-51.
- Muggia F, Kudlowitz D. Novel taxanes. *Anti-cancer drugs.* 2014; 25: 593-8.
- Fulton B, Spencer CM. Docetaxel. *Drugs.* 1996; 51: 1075-92.
- Engels FK, Mathot RAA, Verweij J. Alternative drug formulations of docetaxel: a review. *Anti-Cancer Drugs.* 2007; 18: 95-103.
- Hao Y, Wang L, Zhao Y, Meng D, Li D, Li H, et al. Targeted imaging and chemo-phototherapy of brain cancer by a multifunctional drug delivery system. *Macromol Biosci.* 2015; 15: 1571-85.
- Jain S, Spandana G, Agrawal AK, Kushwah V, Thanki K. Enhanced antitumor efficacy and reduced toxicity of docetaxel loaded estradiol functionalized stealth polymeric nanoparticles. *Mol Pharm.* 2015; 12: 3871-84.
- Liang Z, Yang N, Jiang Y, Hou C, Zheng J, Shi J, et al. Targeting docetaxel-PLA nanoparticles simultaneously inhibit tumor growth and liver metastases of small cell lung cancer. *Int J Pharm.* 2015; 494: 337-45.
- Kataoka K, Harada A, Nagasaki Y. Block copolymer micelles for drug delivery: Design, characterization and biological significance. *Adv Drug Deliv Rev.* 2012; 64: 37-48.
- Nishiyama N, Kataoka K. Current state, achievements, and future prospects of polymeric micelles as nanocarriers for drug and gene delivery. *Pharmacol Ther.* 2006; 112: 630-48.
- Zhang Z, Tan S, Feng S-S. Vitamin E TPGS as a molecular biomaterial for drug delivery. *Biomaterials.* 2012; 33: 4889-906.
- Zhang Z, Mei L, Feng S-S. Vitamin E D- α -tocopheryl polyethylene glycol 1000 succinate-based nanomedicine. *Nanomedicine.* 2012; 7: 1645-7.
- Lee SW, Yun MH, Jeong SW, In CH, Kim JY, Seo MH, et al. Development of docetaxel-loaded intravenous formulation, Nanoxel-PM (TM) using polymer-based delivery system. *J Control Release.* 2011; 155: 262-71.
- SW L, MH Y, SW J, CH I, JY K, MH S, et al. Development of docetaxel-loaded intravenous formulation, Nanoxel-PM™ using polymer-based delivery system. *J Control Release.* 2011; 155: 262-71.
- Wang T, Zhu DW, Liu G, Tao W, Cao W, Zhang LH, et al. DTX-loaded star-shaped TAPP-PLA-b-TPGS nanoparticles for cancer chemical and photodynamic combination therapy. *RSC Adv.* 2015; 5: 50617-27.
- Zhang XD, Dong YC, Zeng XW, Liang X, Li XM, Tao W, et al. The effect of autophagy inhibitors on drug delivery using biodegradable polymer nanoparticles in cancer treatment. *Biomaterials.* 2014; 35: 1932-43.
- Tao W, Zeng XW, Liu T, Wang ZY, Xiong QQ, Ouyang CP, et al. Docetaxel-loaded nanoparticles based on star-shaped mannitol-core PLGA-TPGS diblock copolymer for breast cancer therapy. *Acta Biomater.* 2013; 9: 8910-20.
- Dunwan Z, Wei T, Hongling Z, Gan L, Teng W, Linhua Z, et al. Docetaxel (DTX)-loaded polydopamine-modified TPGS-PLA nanoparticles as a targeted drug delivery system for the treatment of liver cancer. *Acta Biomater.* 2016; 30: 144-54.
- Zhang XD, Yang Y, Liang X, Zeng XW, Liu ZG, Tao W, et al. Enhancing therapeutic effects of docetaxel-loaded dendritic copolymer nanoparticles by co-Treatment with autophagy inhibitor on breast cancer. *Theranostics.* 2014; 4: 1085-95.
- Wang ZY, Wu YP, Zeng XW, Ma YP, Liu J, Tang XL, et al. Antitumor efficiency of D-alpha -tocopheryl polyethylene glycol 1000 succinate-b-poly(epsilon-caprolactone-ran-lactide) nanoparticle-based delivery of docetaxel in mice bearing cervical cancer. *J Biomed Nanotechnol.* 2014; 10: 1509-19.
- Nicolas J, Mura S, Brambilla D, Mackiewicz N, Couvreur P. Design, functionalization strategies and biomedical applications of targeted biodegradable/biocompatible polymer-based nanocarriers for drug delivery. *Chem Soc Rev.* 2013; 42: 1147-235.
- Yang T, Choi M-K, Cui F-D, Kim JS, Chung S-J, Shim C-K, et al. Preparation and evaluation of paclitaxel-loaded PEGylated immunoliposome. *J Control Release.* 2007; 120: 169-77.
- Choi CHJ, Alabi CA, Webster P, Davis ME. Mechanism of active targeting in solid tumors with transferrin-containing gold nanoparticles. *P Natl Acad Sci.* 2010; 107: 1235-40.
- Cho H-J, Yoon HY, Koo H, Ko S-H, Shim J-S, Lee J-H, et al. Self-assembled nanoparticles based on hyaluronic acid-ceramide (HA-CE) and Pluronic® for tumor-targeted delivery of docetaxel. *Biomaterials.* 2011; 32: 7181-90.
- Kumar P, Wu HQ, McBride JL, Jung KE, Kim MH, Davidson BL, et al. Transvascular delivery of small interfering RNA to the central nervous system. *Nature.* 2007; 448: 39-43.
- Huimin X, Xiaoling G, Guangzhi G, Zhongyong L, Ni Z, Quanyin H, et al. Low molecular weight protamine-functionalized nanoparticles for drug delivery to the brain after intranasal administration. *Biomaterials.* 2011; 32: 9888-98.
- Li Y, Zhang H, Zhai G-X. Intelligent polymeric micelles: development and application as drug delivery for docetaxel. *J Drug Target.* 2017; 25: 285-95.
- Arranja AG, Pathak V, Lammers T, Shi Y. Tumor-targeted nanomedicines for cancer theranostics. *Pharmacological Rev.* 2016; 155: 87-95.
- Kunjachan S, Pola R, Gremse F, Theek B, Ehling J, Moeckel D, et al. Passive versus Active Tumor Targeting Using RGD- and NGR-Modified Polymeric Nanomedicines. *Nano Lett.* 2014; 14: 972-81.
- Bertrand N, Leroux JC. The journey of a drug-carrier in the body: An anatomo-physiological perspective. *J Control Release.* 2012; 161: 152-63.
- Radomski A, Jurasz P, Alonso-Escolano D, Drews M, Morandi M, Malinski T, et al. Nanoparticle-induced platelet aggregation and vascular thrombosis. *Br J Pharmacol.* 2005; 146: 882-93.
- Maeda H, Wu J, Sawa T, Matsumura Y, Hori K. Tumor vascular permeability and the EPR effect in macromolecular therapeutics: a review. *J Control Release.* 2000; 65: 271-84.
- Shen HX, Shi SJ, Zhang ZR, Gong T, Sun X. Coating Solid Lipid Nanoparticles with Hyaluronic Acid Enhances Antitumor Activity against Melanoma Stem-like Cells. *Theranostics.* 2015; 5: 755-71.
- Shi SY, Liu YJ, Chen Y, Zhang ZH, Ding YS, Wu ZQ, et al. Versatile pH-response Micelles with High Cell-Penetrating Helical Diblock Copolymers for Photoacoustic Imaging Guided Synergistic Chemo-Photothermal Therapy. *Theranostics.* 2016; 6: 2170-82.
- Shen Y, Jin E, Zhang B, Murphy CJ, Sui M, Zhao J, et al. Prodrugs forming high drug loading multifunctional nanocapsules for intracellular cancer drug delivery. *J Am Chem Soc.* 2010; 132: 4259-65.
- Chu BY, Zhang L, Qu Y, Chen XX, Peng JR, Huang YX, et al. Synthesis, characterization and drug loading property of Monomethoxy-Poly(ethylene glycol)-Poly(epsilon-caprolactone)-Poly(D, L-lactide) (MPEG-PCLA) copolymers. *Sci Rep.* 2016; 6: 15.
- Zhang L, Tan LW, Chen LJ, Chen XX, Long CF, Peng JR, et al. A simple method to improve the stability of docetaxel micelles. *Sci Rep.* 2016; 6: 10.
- Wang CY, Mallela J, Mohapatra S. Pharmacokinetics of Polymeric Micelles for Cancer Treatment. *Curr Drug Metab.* 2013; 14: 900-9.
- Walker DA, Kowalczyk B, de la Cruz MO, Grzybowski BA. Electrostatics at the nanoscale. *Nanoscale.* 2011; 3: 1316-44.
- Reisch A, Runser A, Arntz Y, Mely Y, Klymchenko AS. Charge-Controlled Nanoprecipitation as a Modular Approach to Ultrasmall Polymer Nanocarriers: Making Bright and Stable Nanoparticles. *ACS Nano.* 2015; 9: 5104-16.
- He ZL, Sun Y, Wang Q, Shen M, Zhu MJ, Li FQ, et al. Degradation and Bio-Safety Evaluation of mPEG-PLGA-PLL Copolymer-Prepared Nanoparticles. *J Phys Chem C.* 2015; 119: 3348-62.

48. Richardson T, Hodgett J, Lindner A, Stahmann MA. Action of polylysine on some ascites tumors in mice. *Proc Soc Exp Biol Med.* 1959; 101: 382-6.
49. Blout ER, Bovey F, Goodman M, Lotan N. Peptides, polypeptides and proteins-Proceedings of the Rehovot Symposium. Wiley. 1974; 378-80.
50. Arnold L, Dagan A, Gutheil J, Kaplan N. Antineoplastic activity of poly (L-lysine) with some ascites tumor cells. *P Natl Acad Sci.* 1979; 76: 3246-50.
51. Xing LX, Shi QS, Zheng KL, Shen M, Ma J, Li F, Liu Y, *et al.* Ultrasound-Mediated Microbubble Destruction (UMMD) Facilitates the Delivery of CA19-9 Targeted and Paclitaxel Loaded mPEG-PLGA-PLL Nanoparticles in Pancreatic Cancer. *Theranostics.* 2016; 6: 1573-87.
52. Guan X, Li Y, Jiao Z, Lin L, Chen J, Guo Z, *et al.* Codelivery of antitumor drug and gene by a pH-sensitive charge-conversion system. *ACS applied materials & interfaces.* 2015; 7: 3207-15.
53. Zheng XL, Kan B, Gou ML, Fu SZ, Zhang J, Men K, *et al.* Preparation of MPEG-PLA nanoparticle for honokiol delivery in vitro. *Int J Pharm.* 2010; 386: 262-7.
54. Harada A, Kataoka K. Formation of polyion complex micelles in an aqueous milieu from a pair of oppositely-charged block-copolymers with poly(ethylene glycol) segments. *Macromolecules.* 1995; 28: 5294-99.
55. Liu PF, Yu H, Sun Y, Zhu MJ, Duan YR. A mPEG-PLGA-b-PLL copolymer carrier for adriamycin and siRNA delivery. *Biomaterials.* 2012; 33: 4403-12.
56. Wang C, Wang YJ, Wang YJ, Fan M, Luo F, Qian ZY. Characterization, pharmacokinetics and disposition of novel nanoscale preparations of paclitaxel. *Int J Pharm.* 2011; 414: 251-9.
57. Wang YJ, Chen LJ, Tan LW, Zhao Q, Luo F, Wei YQ, *et al.* PEG-PCL based micelle hydrogels as oral docetaxel delivery systems for breast cancer therapy. *Biomaterials.* 2014; 35: 6972-85.
58. Wang YJ, Wang C, Fu SZ, Liu Q, Dou DY, Lv H, Fan M, *et al.* Preparation of Tacrolimus loaded micelles based on poly(epsilon-caprolactone)-poly(ethylene glycol)-poly(epsilon-caprolactone). *Int J Pharm.* 2011; 407: 184-9.
59. Plimpton S. Fast parallel algorithms for short-range molecular-dynamics. *J Comput Phys.* 1995; 117: 1-19.
60. Sun H, Ren P, Fried JR. The COMPASS force field: parameterization and validation for phosphazenes. *Comput Theor Polym Sci* 1998, 8: 229-246.
61. Han KK, Son HS. On the isothermal-isobaric ensemble partition function. *J Chem Phys.* 2001; 115: 7793-94.
62. Makarewicz T, Kazmierkiewicz R. Molecular Dynamics Simulation by GROMACS Using GUI Plugin for PyMOL. *J Chem Inf Model.* 2013; 53: 1229-34.
63. Chen LJ, Tan LW, Zhang XN, Li J, Qian ZY, Xiang ML, *et al.* Which polymer is more suitable for etoposide: A comparison between two kinds of drug loaded polymeric micelles in vitro and in vivo? *Int J Pharm.* 2015; 495: 265-75.
64. Gou ML, Qu X, Zhu W, Xiang ML, Yang J, Zhang K, *et al.* Bio-inspired detoxification using 3D-printed hydrogel nanocomposites. *Nat Commun.* 2014; 5: 9.
65. Wang YL, Zhao H, Peng JR, Chen LJ, Tan LW, Huang YX, *et al.* Targeting Therapy of Neuropilin-1 Receptors Overexpressed Breast Cancer by Paclitaxel-Loaded CK3-Conjugated Polymeric Micelles. *J Biomed Nanotechnol.* 2016; 12: 2097-111.
66. Garay RP, El-Gewely R, Armstrong JK, Garratty G, Richette P. Antibodies against polyethylene glycol in healthy subjects and in patients treated with PEG-conjugated agents. *Expert Opin Drug Deliv.* 2012; 9: 1319-23.
67. Qi YZ, Chilkoti A. Protein-polymer conjugation-moving beyond PEGylation. *Curr Opin Chem Biol.* 2015; 28: 181-93.
68. Hu KL, Cao S, Hu FQ, Feng JF. Enhanced oral bioavailability of docetaxel by lecithin nanoparticles: preparation, in vitro, and in vivo evaluation. *Int J Nanomed.* 2012; 7: 3537-45.
69. Gong CY, Deng SY, Wu QJ, Xiang ML, Wei XW, Li L, *et al.* Improving antiangiogenesis and anti-tumor activity of curcumin by biodegradable polymeric micelles. *Biomaterials.* 2013; 34: 1413-32